الجمهورية الجزائرية الديمقراطية الشعبية

People's Democratic Republic of Algeria

وزارة التعليم العالي والبحث العلمي

MINISTRY OF HIGHER EDUCATION AND SCIENTIFIC RESEARCH

جامعة الشهيد حمه لخضر الوادي

ECHAHID HAMMA LAKHDAR UNIVERSITY OF EL-OUED

كلية العلوم الطبيعة والحياة

FACULTY OF NATURAL LIFE AND SCIENCES

قسم البيولوجيا الخلوية والجزيئية

Department of Cellular and Molecular Biology

END OF STUDY THESIS

With a view to obtaining the Academic Master's degree in Biological Sciences

Specialty: Applied Biochemistry

THEME

Phytochemically-Mediated Green Synthesis of Ag/ZnO Nanocomposite from *Cucumis sativus* Peels Extract: LC-MS Profiling, Comprehensive Characterization, *In Vitro* Bioactivities, and *In Vivo* Burn Wound Healing Efficacy

Presented by:

Miss: BOUZIANE Djouhaina

Miss: ZEBIDI Oum El Hana

Jury Members:

President: Dr. sasdi hamza	El-Oued University
Examiner: Dr**.** ramdan farah	El-Oued University
Supervisor: Dr. Ibtissam LAIB	MCB El-Oued University

University year: 2025/2026


بسم الله الرحمن الرحيم

THANKS

In the name of Allah, the Most Gracious, the Most Merciful

All praise and gratitude are due to Allah Almighty, who bestowed upon us His grace and blessings, and granted us the strength and determination to accomplish this academic work. We pray to Him for continued guidance,

We would like to express our deepest gratitude and sincere appreciation to Dr.Laib Ibtissam for her valuable guidance, continuous support, and constructive comments, which greatly contributed to the successful completion of this research.

We also extend our heartfelt thanks to our beloved parents for their endless support, encouragement, sincere prayers, and great sacrifices, which have always been a source of inspiration and strength throughout the preparation of this work.

Finally, we would like to express our sincere appreciation to ECHAHID HAMMA LAKHDAR UNIVERSITY OF EL-OUED for providing a supportive academic and scientific environment that greatly contributed to the accomplishment of this work.

الاهـــداء

الحمد لله الذي بنعمته تتم الصالحات وبه تختم الرحلات وتتحقق الأمنيات.

اليوم لا نقف عند نهاية طريق ، بل عند بداية حلم جديد . سنوات مضت بين دراسة وتعب بين سقوط ونهوض، وبين حلم كبر معنا يوما بعد يوم.

لم تكن الرحلة سهلة، لكنها كانت مليئة بالدروس.

صنعت منا أشخاصا أقوى، وأقرب لأحلامنا مما كنا نتصوّر.

أهدي تخرجنا الى :

إلى أمي الحبيبة : مصدر الدعاء والحنان والقوة، إليكِ وحدكِ يُهدى هذا النجاح، لأنكِ كنتِ السبب بعد الله في كل خطوة وصلتُ إليها.

إلى أبي الغالي : سندي وفخري وأمان هذا الطريق،شكرًا لكل تعبٍ وصبرٍ ودعمٍ لا يُنسى، هذا التخرّج ثمرةٌ من ثمار عطائك.

إلى إخوتي وأخواتي : شركاء أيامي وضحكاتي وتفاصيلي الجميلة،

شكرًا لوجودكم الدائم بقربي، ولفرحكم الذي كان دائمًا يزيدني قوة.

إلى أستاذتي الفاضلة: شكرًا لكل علمٍ قدّمتهِ، ولكل نصيحةٍ كانت نورًا في الطريق، كان لتوجيهاتكِ أثرٌ كبير في وصولي لهذا اليوم شكرا لكي على كل مجهوداتك.

إلى أصدقائي الأعزاء: رفاق الطريق واللحظات الصعبة والجميلة،

شكرًا لكل دعمٍ وكلمةٍ طيبة وموقفٍ صادق، ستبقى هذه الذكريات من أجمل ما رافق رحلة التخرّج.

اليوم احتفل بثمرة الجهد ، وغدا ابدأ فصلا جديدا من الطموح والسعي، مؤمنة بأن القادم أجمل وأن ما كتبه الله لنا أعظم مما نحلم به.

اللهم لك الحمد حتى ترضى، ولك الحمد على هذا الإنجاز. وبداية مباركة لمستقبل أنتظره بثقة وأمل.

Abstract

Burn injuries continue to represent a significant global health burden, frequently associated with persistent oxidative stress, dysregulated inflammation, microbial infections, and delayed tissue regeneration. The present study aimed to develop advanced topical formulations for burn wound management by valorizing *Cucumis sativus* (cucumber) peels, an abundant agricultural waste from the El Oued region of Algeria, through green synthesis of Ag/ZnO nanocomposite. LC-MS/MS phytochemical profiling of the *C. sativus* peels aqueous extract identified 22 bioactive secondary metabolites, remarkably dominated by L-proline (90.12%), in addition to potent polyphenols (myricetin, resveratrol), phenolic acids (sinapic and ferulic), and organic acids. These phytoconstituents effectively served as reducing and capping agents, enabling the successful and eco-friendly synthesis of a stable Ag/ZnO nanocomposite. Comprehensive characterization confirmed the formation of a highly crystalline biphasic Ag/ZnO nanocomposite with an average crystallite size of 28.97 ± 0.98 nm, characteristic optical absorption at 365 nm, strong bio-capping by plant-derived functional groups, and porous cauliflower-like morphology with substantial silver content (42.71 wt%). *In vitro* assessments revealed that the green-synthesized Ag/ZnO nanocomposite exhibited markedly superior multifunctional activities compared to the crude peel extract, including excellent total antioxidant capacity (TAC = 55.35 ± 1.7 mg AAE/g), potent anti-inflammatory activity (91.47% inhibition of protein denaturation), good photoprotective capacity (SPF = 24.08), and favorable biocompatibility. Two topical creams (10% C. sativus peels extract cream and 0.1% Ag/ZnO nanocomposite cream) were successfully formulated, demonstrating excellent physicochemical stability, high biocompatibility, and absence of dermal irritation in acute skin safety tests. In an in vivo second-degree burn wound model in Wistar rats, the 0.1% Ag/ZnO nanocomposite cream achieved near-complete wound contraction by days 18–21, significantly outperforming both the 10% peel extract cream and the commercial reference MEBO®. Histopathological examinations confirmed accelerated re-epithelialization, well-organized collagen deposition, enhanced angiogenesis, and reduced inflammatory infiltration, while hematological parameters showed restoration toward normal physiological values.

These findings underscore the successful integration of *Cucumis sativus* phytochemicals with green nanotechnology, establishing a sustainable nanotherapeutic platform for advanced burn wound management while supporting agricultural waste valorization and circular economy principles.

Keywords: *Cucumis sativus* peels, green synthesis, Ag/ZnO nanocomposite, LC-MS/MS, burn wound healing, antioxidant, anti-inflammatory, sustainable nanotechnology, Natural topical cream.

RÉSUMÉ

Les brûlures représentent toujours un fardeau sanitaire mondial important, souvent associé à un stress oxydatif persistant, une inflammation dérégulée, des infections microbiennes et un retard de régénération tissulaire. La présente étude visait à développer des formulations topiques avancées pour la prise en charge des brûlures en valorisant les pelures de Cucumis sativus (concombre), un déchet agricole abondant de la région d'El Oued en Algérie, via la synthèse verte de nanocomposite Ag/ZnO. Le profilage phytochimique par LC-MS/MS de l'extrait aqueux des pelures de C. sativus a identifié 22 métabolites secondaires bioactifs, dominés de manière remarquable par la L-proline (90,12 %), accompagnés de polyphénols puissants (myricétine, resvératrol), d'acides phénoliques (sinapique et férulique) et d'acides organiques. Ces phytoconstituants ont efficacement servi d'agents réducteurs et stabilisants, permettant la synthèse verte réussie et écologique d'un nanocomposite Ag/ZnO stable. La caractérisation complète a confirmé la formation d'un nanocomposite Ag/ZnO biphasique hautement cristallin avec une taille cristallite moyenne de 28,97 ± 0,98 nm, une absorption optique caractéristique à 365 nm, un bio-capping fort par les groupes fonctionnels d'origine végétale, et une morphologie poreuse en chou-fleur avec une teneur élevée en argent (42,71 %). Les évaluations *in vitro* ont révélé que le nanocomposite Ag/ZnO synthétisé par voie verte présentait des activités multifonctionnelles nettement supérieures à celles de l'extrait brut, notamment une excellente capacité antioxydante (TAC = 55,35 ± 1,7 mg AAE/g), une activité anti-inflammatoire puissante (91,47 % d'inhibition de la dénaturation des protéines), une bonne capacité photoprotectrice (SPF = 24,08) et une biocompatibilité favorable. Deux crèmes topiques (crème à 10 % d'extrait de pelures de C. sativus et crème à 0,1 % de nanocomposite Ag/ZnO) ont été formulées avec succès, démontrant une excellente stabilité physico-chimique, une biocompatibilité élevée et l'absence d'irritation cutanée lors des tests de sécurité dermique. Dans un modèle in vivo de brûlure au second degré chez le rat Wistar, la crème à 0,1 % de nanocomposite Ag/ZnO a permis une contraction quasi complète de la plaie entre les jours 18 et 21, surpassant significativement la crème à 10 % d'extrait de pelures et la référence commerciale MEBO®. Les examens histopathologiques ont confirmé une ré-épithélialisation accélérée, un dépôt organisé de collagène, une angiogenèse améliorée et une infiltration inflammatoire réduite, tandis que les paramètres hématologiques ont montré un retour vers les valeurs physiologiques normales.

Ces résultats soulignent l'intégration réussie des composés phytochimiques de *Cucumis sativus* avec la nanotechnologie verte, établissant une plateforme nanothérapeutique durable pour la prise en charge avancée des brûlures, tout en favorisant la valorisation des déchets agricoles et les principes d'économie circulaire.

Mots-clés : Pelures de *Cucumis sativus*, synthèse verte, nanocomposite Ag/ZnO, LC-MS/MS, cicatrisation des brûlures, antioxydant, anti-inflammatoire, nanotechnologie durable, crème topique naturelle.

الملخص

لا تزال إصابات الحروق تُشكّل عبئًا صحيًا عالميًا كبيرًا، وغالبًا ما ترتبط بالإجهاد التأكسدي المستمر، والالتهاب غير المنتظم، والعدوى الميكروبية، وتأخر تجدد الأنسجة. هدفت هذه الدراسة إلى تطوير تركيبات موضعية متقدمة لعلاج جروح الحروق من خلال الاستفادة من قشور الخيار (Cucumis sativus)، وهي نفايات زراعية وفيرة من منطقة الوادي في الجزائر، وذلك عبر التخليق الأخضر لمركب نانوي من الفضة/أكسيد الزنك. كشف التحليل الكيميائي النباتي باستخدام تقنية LC–MS/MS للمستخلص المائي لقشور الخيار عن 22 مستقلبًا ثانويًا نشطًا بيولوجيًا، يهيمن عليها بشكل ملحوظ L–برولين (90.12%)، بالإضافة إلى مركبات البوليفينول القوية (الميريسيتين، والريسفيراترول)، والأحماض الفينولية (حمض السينابينيك وحمض الفيروليك)، والأحماض العضوية. عملت هذه المكونات النباتية بفعالية كعوامل اختزال وتثبيت، مما مكّن من التخليق الناجح والصديق للبيئة لمركب نانوي مستقر من الفضة/أكسيد الزنك. أكدت دراسة شاملة لخصائص المركب النانوي Ag/ZnO ثنائي الطور عالي التبلور، بمتوسط حجم بلوري يبلغ 28.97 ± 0.98 نانومتر، وامتصاص ضوئي مميز عند 365 نانومتر، وتغليف حيوي قوي بواسطة مجموعات وظيفية مشتقة من النباتات، وبنية مسامية تشبه القرنبيط مع محتوى كبير من الفضة (42.71% وزناً). وكشفت التقييمات المخبرية أن المركب النانوي Ag/ZnO المُصنّع بطريقة صديقة للبيئة أظهر أنشطة متعددة الوظائف فائقة بشكل ملحوظ مقارنةً بمستخلص القشرة الخام، بما في ذلك قدرة مضادة للأكسدة كلية ممتازة (TAC = 55.35 ± 1.7 ملغ مكافئ حمض الأسكوربيك/غرام)، ونشاط قوي مضاد للالتهابات (91.47% تثبيط لتشوه البروتين)، وقدرة جيدة على الحماية من الضوء (SPF = 24.08)، وتوافق حيوي جيد. تم بنجاح تحضير نوعين من الكريمات الموضعية (كريم مستخلص قشور نبات C. sativus بتركيز 10% وكريم مركب نانوي من الفضة/أكسيد الزنك بتركيز 0.1%)، وقد أظهرت هذه الكريمات استقرارًا فيزيائيًا وكيميائيًا ممتازًا، وتوافقًا حيويًا عاليًا، وعدم تسببها في تهيج الجلد في اختبارات السلامة الجلدية الحادة. في نموذج حيواني لحروق من الدرجة الثانية في فئران ويستار، حقق الكريم المركب النانوي من الفضة/أكسيد الزنك بتركيز 0.1% انكماشًا شبه كامل للجرح في غضون 18–21 يومًا، متفوقًا بشكل ملحوظ على كل من كريم مستخلص القشور بتركيز 10% والكريم المرجعي التجاري MEBO®. أكدت الفحوصات النسيجية المرضية تسارع إعادة تكوين الظهارة، وترسب الكولاجين بشكل منظم، وتعزيز تكوين الأوعية الدموية، وانخفاض التسلل الالتهابي، بينما أظهرت المؤشرات الدموية عودة إلى القيم الفسيولوجية الطبيعية.

تؤكد هذه النتائج على التكامل الناجح للمواد الكيميائية النباتية لنبات الخيار (Cucumis sativus) مع تكنولوجيا النانو الخضراء، مما يؤدي إلى إنشاء منصة علاجية نانوية مستدامة لإدارة جروح الحروق المتقدمة مع دعم تثمين النفايات الزراعية ومبادئ الاقتصاد الدائري.

الكلمات المفتاحية: قشور الخيار، التخليق الأخضر، مركب النانو Ag/ZnO، LC–MS/MS، التئام جروح الحروق، مضادات الأكسدة، مضادات الالتهاب، تقنية النانو المستدامة، كريم موضعي طبيعي.

Content

First part

Bibliographic synthiesis

CHAPTER 1 :

An overview of the cucumber plant

CHAPTER 2:

Ag-ZnO Nanoparticles

Second part :

CHAPTER 1:

Materials And Methods

List of figure

List of table

Liste of Abbreviation

Abs**: Absorbance**

DMSO**: dimethyl sulfoxyl**

C.sativus**: Cucumis sativus**

DPPH**: 2,2-diphenyl-1-1-picrylhdrqwyl**

EC_{50}**: Median effective concentration**

EDT: **Ethylenediaminetetraacetic acid**

FRAP: **Ferric reducing antioxidant power**

HPLC**: High-performance liquid chromatography**

LC-MS**: Liquid Chromatography-Tandem Mass Spectrometry**

IC_{50}**: Inhibitory concentration 50**

PBS**: Phosphqte-buffered saline**

*B.suptilis***: Bacillus suptilis**

*K.pneumoniae***: Klebsiella pneumoniae**

*E.coli***: Echerichia coli**

SDS**: Sodium**

SPF**: Sun protection factor**

TAC**: Total antioxidant capacity**

UV-VIS**: Ultraviolet Visible**

XRD**: X-ray diffraction**

SEM**: Scanning electron microscopy**

EDX**: dispersive spectroscopy**

General Introduction

Burns represent one of the most devastating forms of traumatic injury, constituting a major global public health concern associated with high morbidity, mortality, and significant socio-economic burden. According to the World Health Organization (2023), approximately 180,000 deaths occur annually due to burn injuries, with the vast majority occurring in low- and middle-income countries. Beyond mortality, non-fatal burns often result in long-term physical disabilities, hypertrophic scarring, contractures, psychological trauma, and reduced quality of life for survivors and their families (Jeschke *et al*., 2020; Smolle *et al*., 2022).

The management of burn wounds remains a considerable clinical challenge. Conventional treatments, including silver sulfadiazine, topical antibiotics, and advanced dressings, frequently encounter limitations such as delayed healing in deep burns, emergence of antimicrobial resistance, excessive scar formation, and potential cytotoxicity (Oaks et al., 2023; Khansa *et al*., 2019). These shortcomings underscore the urgent need for innovative, effective, safe, and affordable therapeutic strategies capable of addressing the complex pathophysiology of burn wounds, which involves prolonged inflammation, severe oxidative stress, impaired angiogenesis, and high susceptibility to infection.

In response to these challenges, the scientific community has increasingly turned toward natural resources and green nanotechnology. Agricultural waste valorization has emerged as a sustainable strategy that transforms low-value by-products into high-value bioactive materials. Among such resources, cucumber peels (*Cucumis sativus* L.), often discarded as waste, represent a promising and underexplored candidate. Cucumber peels are rich in bioactive secondary metabolites, including polyphenols, flavonoids (such as kaempferol, quercetin, and myricetin), phenolic acids, vitamins, and amino acids like L-proline. These compounds confer potent antioxidant, anti-inflammatory, antimicrobial, and tissue-regenerative properties (Priyadarshini et al., 2020; Ramadhani *et al*., 2023; Khan *et al*., 2022).

Parallel to phytotherapy, nanotechnology has revolutionized wound care. In particular, silver-zinc oxide (Ag/ZnO) nanocomposites have gained considerable attention due to their synergistic biological activities. The incorporation of silver nanoparticles enhances broad-spectrum antimicrobial efficacy, while zinc oxide contributes antioxidant, anti-inflammatory, and pro-regenerative effects through controlled ion release and ROS modulation. When combined, these two components exhibit superior performance compared to their individual

counterparts in promoting wound closure, collagen deposition, angiogenesis, and re-epithelialization (Rafique *et al*., 2024; Zhao *et al*., 2024).

To overcome the environmental and toxicological drawbacks associated with conventional chemical synthesis, green synthesis using plant extracts has become the preferred approach. Plant-derived phytochemicals (phenolics and flavonoids) serve simultaneously as reducing, capping, and stabilizing agents, yielding biocompatible, eco-friendly, and cost-effective nanoparticles with enhanced biological activity (Akbar Ali *et al*., 2019; Marslin *et al*., 2018).

Despite the individual therapeutic potential of *Cucumis sativus* peels and Ag/ZnO nanoparticles, limited research has explored their integrated application in the form of a topical formulation for burn wound management. Furthermore, studies utilizing locally sourced Algerian cucumber peels for the green synthesis of Ag/ZnO nanocomposites and their subsequent evaluation in experimental burn models remain scarce. This represents a significant research gap, particularly in the context of sustainable development and circular economy principles through the valorization of agricultural waste.

The present work aims to bridge this gap by developing a novel bioactive cream based on the green synthesis of Ag/ZnO nanocomposite using aqueous *Cucumis sativus* peels extract, followed by comprehensive physicochemical characterization and evaluation of its therapeutic efficacy in a rat model of burn wounds.

Research Objectives:

Part One: To study cucumber (*Cucumis sativus*) and its peels, including their chemical composition, wide traditional and medicinal applications, and their valorization in green synthesis.

Part Two: To review the properties, mechanisms of action, and applications of zinc-silver nanocomposite in wound healing.

Practical Part:

- ✓ To characterize the phytochemical profile of *C. sativus* peels aqueous extract using qualitative, quantitative, and LC-MS/MS analyses.
- ✓ To synthesize and fully characterize Ag/ZnO nanocomposite using the cucumber peel extract as both reducing and capping agent (UV-Vis, FTIR, XRD, and SEM-EDX).
- ✓ To formulate stable topical creams incorporating the plant extract and the green-synthesized Ag/ZnO nanocomposite.

- ✓ To assess the *in vitro* antioxidant, anti-inflammatory, photoprotective, and antibacterial activities of the developed formulations.
- ✓ To evaluate the *in vivo* wound healing efficacy, histological improvements, hematological effects, and biosafety of the formulations in an experimental burn wound model in Wistar rats, compared to commercial standards.

This study is expected to provide a scientifically validated, sustainable, and cost-effective therapeutic alternative for burn wound management while promoting the valorization of agricultural by-products in accordance with green chemistry principles.

First part :

Bibliographic synthiesis

CHAPTER I :

An overview of the cucumber plant

1. Generality

Cucumber is originated from india,particularly southern foot-hills of himalaya region.It was domesticated in India from its wild relative;*Cucumis sativus* var. 3000 years ago. It is commercially grown in the tropical and cuptropical regions of the world.The fruits are widly consumed as salad at immature stage. Cucumber probably originated in India from where it seems to have spread Eastwards to China and westwards to Asia Minor, North Africa and Southern Europe and subsequently to entire plante dit in Haiti in 1494and perhaps soon afterwards it was brought to the USA. Cucumber was domesticated about 3000 years ago and is indigenous to India, (primary centre of diversity). *C. sativus* var is a wild relative. This botanical variety is sympatric and cross-compatible with *Cucumis sativus* var sativus and has multiple fruiting and branching habit which is uncommon in cucumber. As against India which is the primary centre of diversity of cucumber, China is concidered as secondary centre of diversity. The cucumber originates from South Asia, but now grows on most continents, as many different types of cucumber are traded on the global market. Cultivated for at least 3,000 years,the cucumber originated from India,where a great many varieties have been observed, along with its closest living relative, *Cucumis hystrix.* It was probably introduced to Europe by the Greeks or Romans.(Swamy.K.R.M., 2023).

2.Botanical description

Cucumbers *(Cucumis sativus* var.spp) are botanically categorized as berries, which are available in many different sizes shapes and colors. They range from thick, stubby little fruits (10-12 cm long) to dutch greenhouse varieties (of up to 50 cm long).the most popular variety is the long smooth salad cucumber which has a smooth,dark-green skin.Its brother,the "gherkin" is actually a cucumber that has been harvested when little and pickled in brine. The true gherkinis a different species (*Cucumis anguria*), which is primarily grown in the West Indies. Cucumber may not contain a lot of food value,but they make up this lack of nutrients with a wide variety of healthy substances.(Sahu T.,Sahu J., 2015).

3. Morphology of Cucumber

Plant: The cucumber; *Cucumis sativus*, is a creeping vine (climbing or sprawling) that roots in the ground and grows up trellises on other supporting frames, wrapping around ribbing with thin, spiraling tendrils. Cucumber plants are annual plants, surviving only one growing season and the vines can reach up to 5 m in length.the plant may have 4 or 5 main stems from which the tendrils branch. (Long An., 2015)

Leaves: The plant has large leaves that form a canopy over the fruit. The leaves of the plant are arranged alternately on the vines, have 3-7 pointed lobes and are hairy; branched tendrils at leaf axes supportclimbing. (Long An., 2015)

Flowers: Cucumber plants are tendril bearing vines with triangular prickly hairy leaves and yellow flowers which are either male or female. The male flowers are in clusters with short, slender pedicels.The Female flowers are usually solitary with stout,short pedicels.Female flowers are yellow with 5 petals. (Long An., 2015)

Seed: Cucumber seeds are much smaller than Pumpkin seeds, relatively narrower and thicker and with almost no marginal groove. The cucumber is a creeping vine that roots in the ground and grows up trellises or other supporting frames. **(Long An., 2015)**

Figure 1: Morphological characteristics of Cucumis sativus (Cucumber plant). (a) Whole plant with fruits (b): Mature cucumber fruit (c): Yellow flower (d) :Leaves and flower.(Swam K.R.M., 2023).

4.Taxonomy and Classification

Bitter gourd belongs to Family :Cucurbitaceae, Subfamily:Cucurbitoideae, Tribe: Melothrieae, Subtribe:Cucumerinae, Genus:Cucumis and Species:*Cucumis sativus L*. Cucumis in Latin means 'Cucumber',the word was derived from Greek for cucumber,hykyon. The epithet sativus, also Latin,means'that is sown',referring to the common agricultural use of the species.Common Names of Cucumber are garden cucumber, apple cucumber, gherkin,concomber (French), cornichon (French),pepino (Spanish and portuguese),huang gua (pinyin,China), khira(Pakistan).which classifies cucumber as follows:(Swamy,2023) .(Sahu T, Sahu J., 2015).

Table 1: Taxonomic Classification of Cucumis sativus L.

Rank	Classification
Kingdom	Plantae
Phylum	Tracheophyta
Class	Magnoliopsida
Order	Cucurbitales
Family	Cucurbitaceae
Genus	Cucumis
Species	*Cucumis sativus* L.
Botanical Name	*Cucumis sativus* Linn.
English Name	Cucumber
Hindi Name	Khira / Kheera

5.Secondary Metabolism and phytochemical Analysis of *C.sativus Peels* Extracts

Secondary metabolites are specialized bioactive molecules synthesized by plant to enthance their competitive fitness within their respective environments.With over 50,000 compounds discovred to date,these metabolites exert profound effects on plant physiology-regulating flowing,fruit set, and growth patterns-while also serving as critical defense mechanisms against microbial pathogens and environmental stressors.Consequently,these compounds from thepharmacological basis for both traditional herbal medicine and modern therapeutics.Recent advanced analytical investigations into the peels of cucumber (*Cucumis sativus L*) utilizing High-Performance Liquid Chromatography coupled with Electrospray lonization Quadrupole Time-of-Flight Mass Spectrometry (UPLC-ESI-Q-Tof-MS) have

unveiled a complex chemical profile.Research by (Mansfeld *et al*., 2017)identified thousands of ion peaks,including unique terpenoid glycosides and 210 flavonoid metabolites. Notably, the differential accumulation of anthocyanins (such as cyanidin 3-O-galactoside) and chalcones during advanced growth stages (12-30 days post-pollination) has been linked toimproved resistance.Complementary studies by (abbas *et al*., 2022)on methanolic extracts further characterized six major phenolic compounds,includingcaffeic,gallic,chlorogenenic,and vanillic acids.Among these,kaempferol was identified as a dominat constituent, underscoring the extract.Furthermore,analysis of specific lines (e.g., the PW line) corrborated the presence of a diverse array of flavonols, isoflavonols,and anthocyanine.Collectively, these findings provide a robust scientific foundation for the therapeutic application of *C.sativus Peels* extracts , particularly as antioxidant and tissue-regenerating agents.

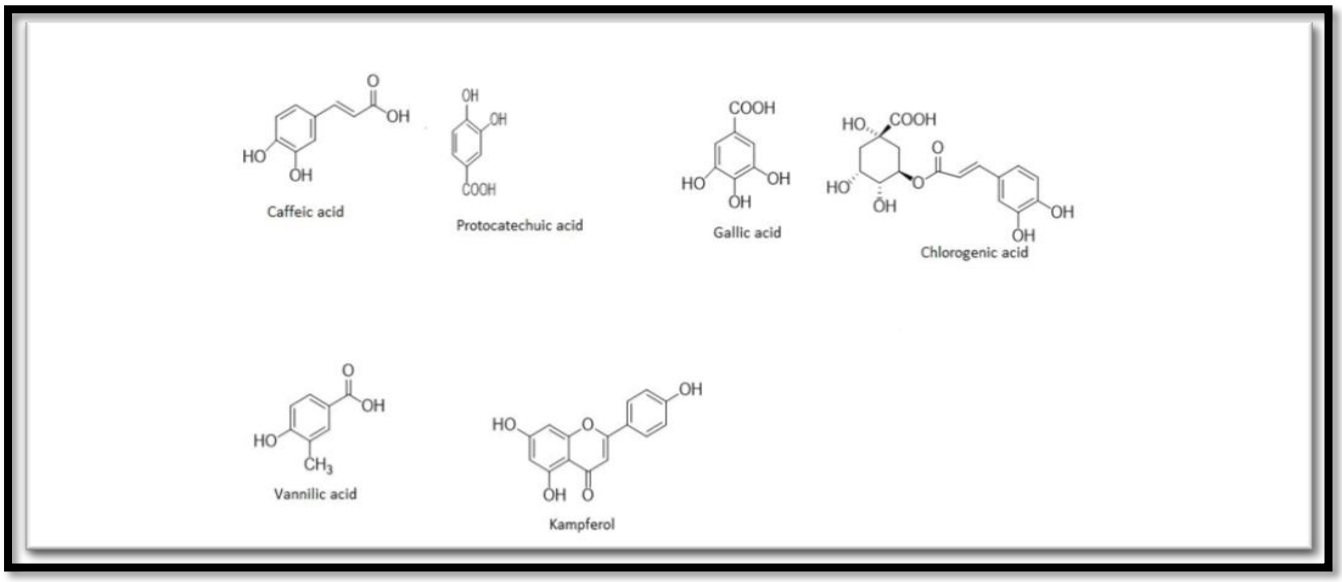

Figure 2: Principal Phenolic and Flavonoid compounds Identified in *C.sativus* Peels .(Khalid Hamid *et al*., 2022).

6.Therapeutic uses of *C.sativus Peels*

6.1.Antipyretic activity

On the peel of cucumber (*Cucumis sativus Linn*) showed the active compounds of saponins, phenolics,steroids,protein,calium and flavonoids.From the overall results of observation, it can be concluded that administration of methanol extract of *C.sativus Peels* to test animals induced by peptones can result in a decrease in temperature. This shows that in the *C.sativus Peels* there are compounds that can reduce temperature, the substances that play a role are flavonoids.(Arfianto N.Saputri.C,A *et al*., 2024).

6.2.Antioxidant activity

C.sativus Peels (*Cucumis sativus L.*) are considered a rich and concentrated source of biologically active compounds with potent antioxidant properties, as they contain a higher eatio of phenolic compounds and flavonoids compared to the fruit pulp. The efficacy of these peels has been proven in vitro through various biological assays, such as the DPPH test (D.P.P.H. radical scavenging assay), where the extracts recorded the highest free radical scavenging activity, reaching up to 71%. These results confirm that the chemical composition of the peels, supported by active substances like vitamin C (Ascorbic Acid), grants them a high reduction capability and the ability to combat oxidative stress, making them a strong candidat for use as a natural antioxidant in food and pharmaceutical application.(Priyadarshini ,Monica S. J *et al*., 2020).

6.3.Antimicrobial activity and acne treatment

The study proved that the ethanol extract of *C.sativus Peels* (*Cucumis sativus L.*) possesses a very strong antimicrobial activity against Staphylococcus epidermidis bacteria, which is one of the main causes of acne. This activity is attributed to the *C.sativus Peels* containing a group of active secondary metabolites such as flavonoids, phenols, steroids, alkaloids, and saponins. The efficacy test of the crude extract specifically showed that the Minimum Bactericidal Concentration (MBC) is 5%. When this extract was formulated into an anti-acne cream, the formulation showed excellent efficacy, registering wide inhibition zones ranging from 33.00 mm to 52.70 mm against the mentioned bacteria, which confirms the scientific basis for using *C.sativus Peels* as a natural, effective topical treatment for acne cases.(Ramadhani N.W,Bintari S.H., 2023).

CHAPTER II:

Ag-ZnO Nanoparticles

1. Nanotechnology

Nanotechnology is a fundamental pillar of modern technological advancement, centered on manipulating material properties at a scale of 10^-9 meters. This field transcends mere miniaturization to encompass the engineering of molecular systems and the integration of nanomaterials to achieve superior functionalities. Innovations in nanomaterials, particularly carbon-based ones, have catalyzed a paradigm shift in medical and technical applications. By exploiting the unique physical and chemical characteristics of nanostructures, current research seeks to address complex environmental and technical challenges such as renewable energy conversion and water purification, positioning nanotechnology as a promising field for developing sustainable and highly efficient solutions.(Mahmoud Nasrollahzadeh *el al*., 2019)

2. Metal Nanoparticles

Metal nanoparticles are widely investigated because of their unique physicochemical and functional properties. **.(Hosny *S et al*., 2025)**

2.1 Silver Nanoparticles

Silver nanoparticles are widely recognized for their unique physicochemical properties, such as high surface-area-to-volume ratio, electrical conductivity, and plasmonic behavior, which make them suitable for a variety of applications. Their ease of synthesis via both chemical and green routes, cost-effectiveness, and broad-spectrum antimicrobial activity have driven their integration into biomedical, environmental, and industrial domains.(Hosny S *et al*., 2025)

2.2 Zinc Oxide Nanoparticles

ZnO is described as a functional, strategic, promising, and versatile inorganic material with a broad range of applications. It is known as a II-VI semiconductor, since Zn and O are classified into groups two and six in the periodic table, respectively. ZnO holds unique optical, chemical sensing, semiconducting, electrical conductivity, and piezoelectric properties. It is characterized by a direct wide band gap (3.3 eV) in the near-UV spectrum, a high excitonic binding energy (60 meV) at room temperature, and a natural n-type electrical conductivity. These characteristics significantly affect its electrical conductivity and optical absorption. The synthesis of nano-sized ZnO has led to the investigation of its use as a new antibacterial agent. In addition to its unique antibacterial and antifungal properties, ZnO-NPs possess high catalytic and photochemical activities. ZnO possesses high optical absorption in the UVA (315–400 nm) and UVB (280–315 nm) regions, which is beneficial in antibacterial response and allows use as a UV protector in cosmetics.(Amna S irelkhatim *et al*., 2015).

3. Various Methods for the Synthesis of Metal Nanoparticles

Metal NPs are generally obtained using nanotechnology by reducing the respective metal to nanoscale size. Their synthesis can be performed using physical, chemical, and biological techniques.(Ana Flavia Burlec *et al*., 2023)

3.1 Physical Methods

Physical approaches prevent NPs from becoming contaminated with solvents but need a significant amount of energy for condensation and evaporation. High modulation of temperature and pressure also raises the cost of synthesis. .(Ana Flavia Burlec *et al*., 2023)

3.2 Chemical Methods

In chemical engineering, reducing and protective agents are used for the synthesis of NPs and agglomeration is prevented, thus generating NPs with high purity and stability. However, contamination can be caused by a significant number of strong chemicals.(Ana Flavia Burlec., 2023)

3.3 Biological Methods

The interest in the biological synthesis of NPs is based on the fact that it offers an eco-friendly and effective alternative to chemical and physical methods. The biological technique employed in green synthesis varies depending on the type of reducing agent used, such as microorganisms (bacteria and fungi) and plants. .(Ana Flavia Burlec., 2023)

4. Green Synthesis of Nanoparticles

One of the most cost-effective and environmentally friendly methods of synthesizing metal NPs is through the use of plants, which act as biofactories for NP production. The potential scale-up of metal NPs obtained using plants is immense due to their abundance, easy availability, and ability to be grown under diverse environmental conditions. Additionally, plant-based synthesis eliminates the need for expensive and hazardous chemicals typically used in conventional methods, making it a safer and more sustainable option. However, drawbacks include variability in size and shape due to differences in plant species, growth conditions, and harvesting times. Nonetheless, recent studies have reported yields of up to several grams of NPs per kilogram of plant material, making plant-based NP synthesis a viable option for industrial-scale production. Consequently, synthesis using plant extracts is an interesting alternative for the large-scale manufacturing of NPs and has great potential for medical applications.(Akbar Ali *et al*., 2019).

5. Mechanism of Green Synthesis of Ag-ZnO by Plant Extracts

The photocatalytic mechanism of the Ag-ZnO nanocomposite relies on enhancing charge separation efficiency and suppressing recombination of electron-hole pairs. Upon

exposure to ultraviolet radiation with energy equal to or exceeding its band gap, electrons in ZnO are excited from the valence band to the conduction band, leaving positively charged holes. In this binary system, silver acts as a chemical trap that captures photo-generated electrons, preventing recombination. The trapped electrons reduce dissolved oxygen to produce superoxide radicals, while the holes react with water molecules or hydroxyl ions to generate hydroxyl radicals. These radicals facilitate oxidation of organic pollutants into harmless substances such as carbon dioxide and water.**(Amna Sirelkhatim *et al.*, 2015)(Shimaa Hosny *et al.*, 2025)**

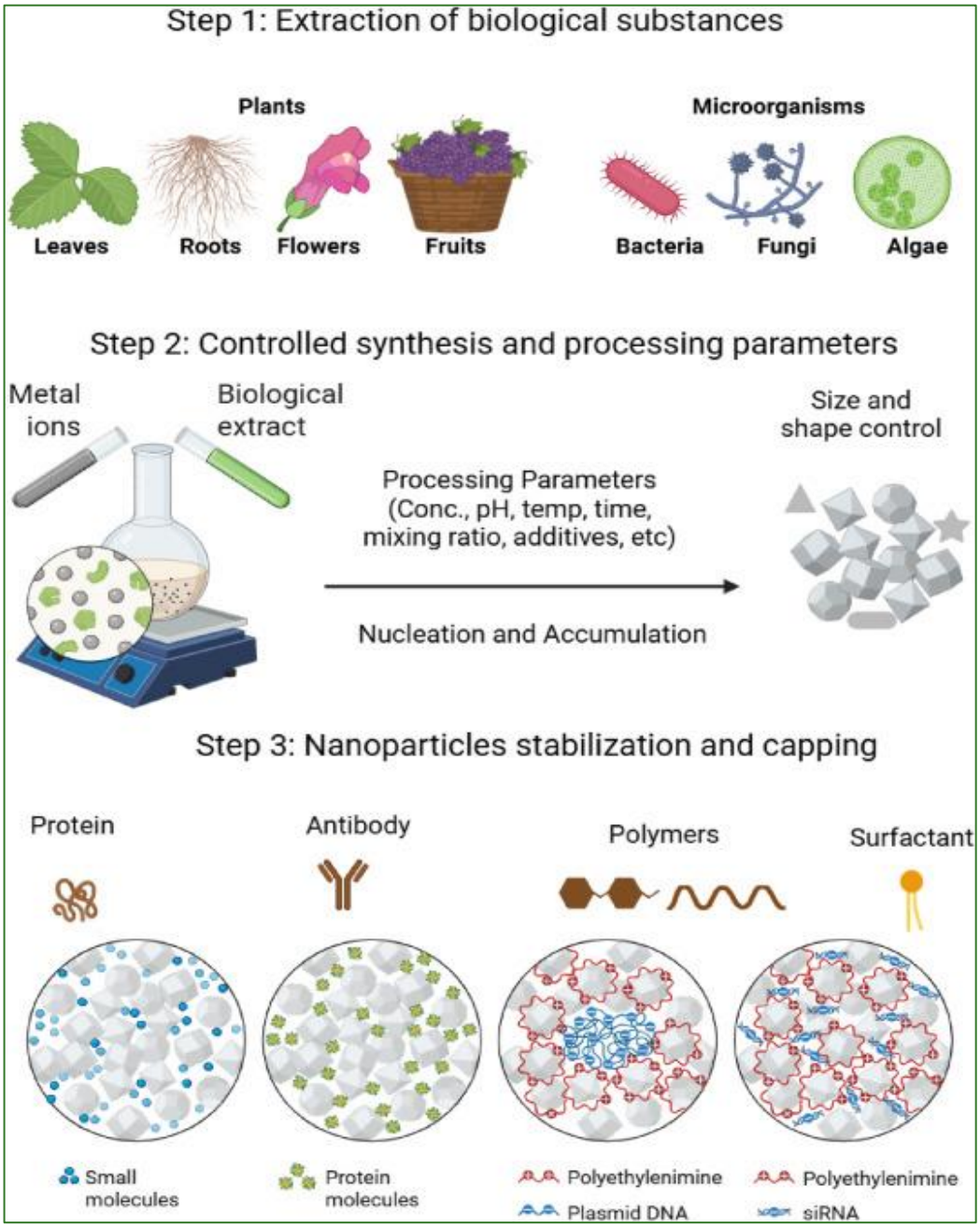

Figure 3: Green Synthesis Mechanism of Ag/ZnO Nanoparticles Using Plant Extracts.(Ibtissam Laib *et al.*, 2025).

6. Secondary Metabolites in Plant Extract-Mediated Green Synthesis of Ag-ZnO

The green synthesis of the Ag/ZnO nanocomposite is fundamentally driven by the dual role of secondary metabolites derived from botanical sources. These compounds, primarily phenolics, flavonoids, and alkaloids, function as reducing agents that transform metal ions into stable nanoparticles. Simultaneously, they act as capping agents that prevent agglomeration by binding to the surface and providing steric and electrostatic stabilization.(Gregory Marslin *et al*., 2018).

7. Characterization Techniques of Nanoparticles

7.1. UV-Visible Spectrophotometer

Used to determine wavelengths and optical properties of obtained compounds.(Ben Dani H, Ghattas D., 2024)

7.2 Scanning Electron Microscopy (SEM)

SEM allows imaging objects at submicron and nanoscale dimensions, enabling morphological analysis and surface characterization. .(Al Shammari,A.A. (Year). Science:Nanotechnology and Nanocience.Publisher)

7.3. Fourier-Transform Infrared Spectroscopy (FTIR)

FTIR measures interaction of infrared radiation with matter and is used to identify functional groups and chemical bonds.(Al Shammari,A.A. (Year). Science:Nanotechnology and Nanocience.Publisher)

7.4 X-ray Diffraction (XRD)

Provides information about crystalline nature, lattice symmetry, unit cell structure, and electron density. (Ben Dani H, Ghattas D., 2024)

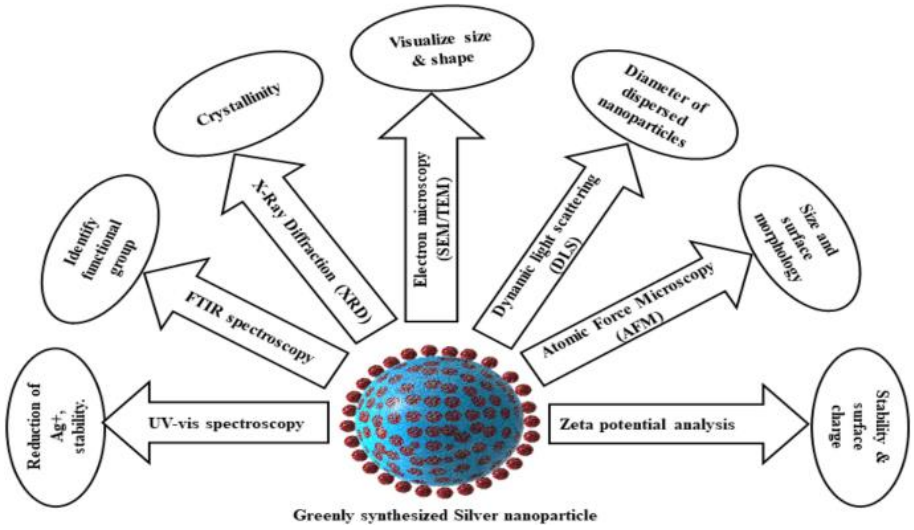

Figure 4:Role of Plant Secondary Metabolites in Green Synthesis of Ag/ZnO Nanoparticles and Characterization Methods (UV-VIS,SEM, FTIR,XRD).(Nancy Jain *et al*., 2021).

8. Biological Applications of Ag-ZnO Nanocomposites

The integration of Ag and ZnO into a single nanocomposite creates a synergistic effect that significantly enhances biological performance compared with individual forms.

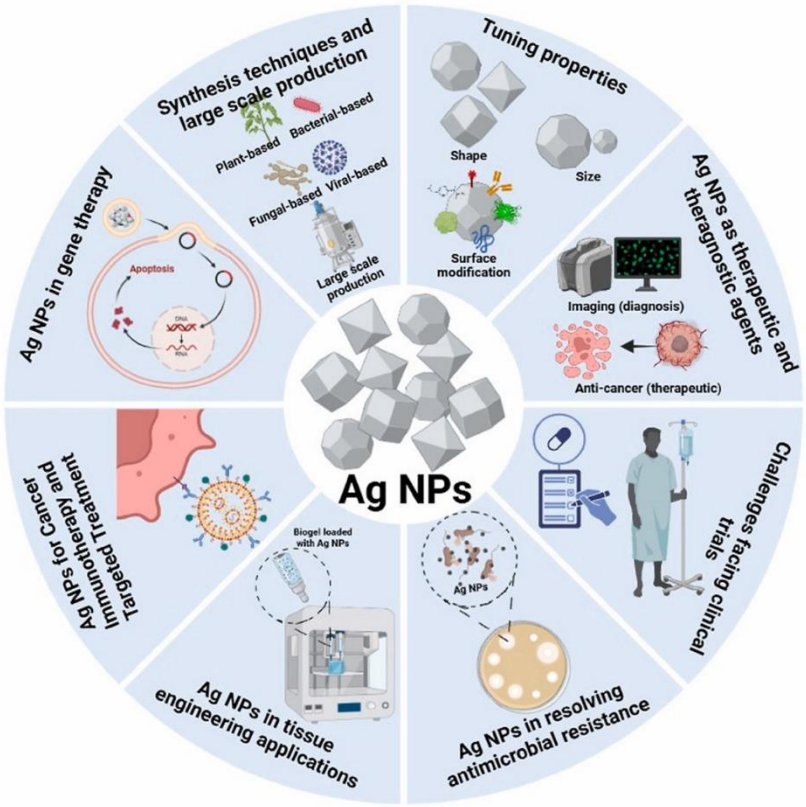

Figure 5:Applications of Silver Nanoparticles(AgNPs) in Medicine: Synyhesis, Modification, and Therapeutic Uses.(Ibtissam Laib *et al*., 2025).

8.1.Anticancer Activities

The hybrid zinc oxide/silver nanoparticles (ZnO/Ag) operate through multiple integrated mechanisms to combat cancer cells, with the additional feature of being able to function as both diagnostic and therapeutic agents (theranostic agents) (Ghaemi *et al*., 2018). The first mechanism is the induction of oxidative stress via reactive oxygen species (ROS) , where coating silver nanoparticles with zinc oxide leads to the regulation of electron flow and the formation of active photogenerated holes; under ultraviolet light irradiation, the photocatalytic activity is stimulated, generating free radicals such as hydroxyl radicals and hydrogen peroxide, and these radicals cause severe oxidative stress leading to damage to DNA, proteins, and mitochondria (Ghaemi *et al*., 2018). This system is characterized by the nanoparticles being non-toxic to normal cells in the dark, highlighting their biocompatible properties when not exposed to light excitation (Ghaemi *et al*., 2018). The second mechanism is the activation of the apoptotic cell death pathway via the mitochondrial pathway, where the

nanoparticles increase the gene expression of pro-apoptotic proteins such as Bax, p53, caspase-3, caspase-9, Cytochrome c, and Apaf-1, with a decrease in the Bcl2 ratio (anti-apoptotic protein), thereby increasing the Bax/Bcl2 ratio in favor of cell death.Studies have shown an increase in p53 gene expression of up to 10,380-fold when using concentrated doses of S. pachycarpa Ag-doped ZnO nanoparticles .The third mechanism is the inhibition of the PI3K/AKT/mTOR pathway, where Ag/ZnO nanoparticles inhibit the production of key proteins in this pathway responsible for cancer cell growth and division, leading to inhibition of cell growth and cell cycle arrest by reducing the expression of proteins such as Cyclin D and CDK .The fourth mechanism is mitochondrial dysfunction, where the nanoparticles reduce the mitochondrial membrane potential (MMP), leading to loss of mitochondrial function, followed by the release of cytochrome c into the cytoplasm, which stimulates the activation of caspase-9 and caspase-3 via the intrinsic apoptosis pathway .The fifth mechanism is diagnostic and imaging capabilities, where Ag/ZnO nanoparticles act as contrast agents enhanced for computed tomography (CT) and optical imaging of cancer cells, making them both therapeutic and diagnostic agents (Ghaemi *et al*., 2018). The key to the efficiency of these nanoparticles lies in the synergistic effect between the silver and zinc components, as studies have shown that ZnO-Ag NPs achieve a lower IC50 value (i.e., greater efficacy) compared to ZnO NPs alone; for NCI-H460 lung cancer cells, the IC50 was 30 µg/mL for ZnO-Ag NPs compared to 40 µg/mL for ZnO NPs alone (Goel *et al*., 2024). Experiments on different types of cancer have shown promising results: in breast cancer (MDA-MB231), Ag/ZnO nanoparticles achieved 99% inhibition of cells upon photoactivation (Ghaemi et al., 2018); in cervical cancer (HeLa), the IC50 was 58 ± 2.9% at a concentration of 5 µg/mL with significant inhibition of the PI3K/AKT/mTOR pathway (Anonymous., 2024); and in multiple myeloma (U266B1), the IC50 was 585 µg/mL with a 10,380-fold increase in p53 expression.These nanoparticles are distinguished from conventional therapies by having multiple mechanisms of action simultaneously, and their activation can be optically controlled to reduce toxicity to healthy cells, making them strong candidates for personalized medicine and smart cancer therapy (Ghaemi *et al*., 2018).

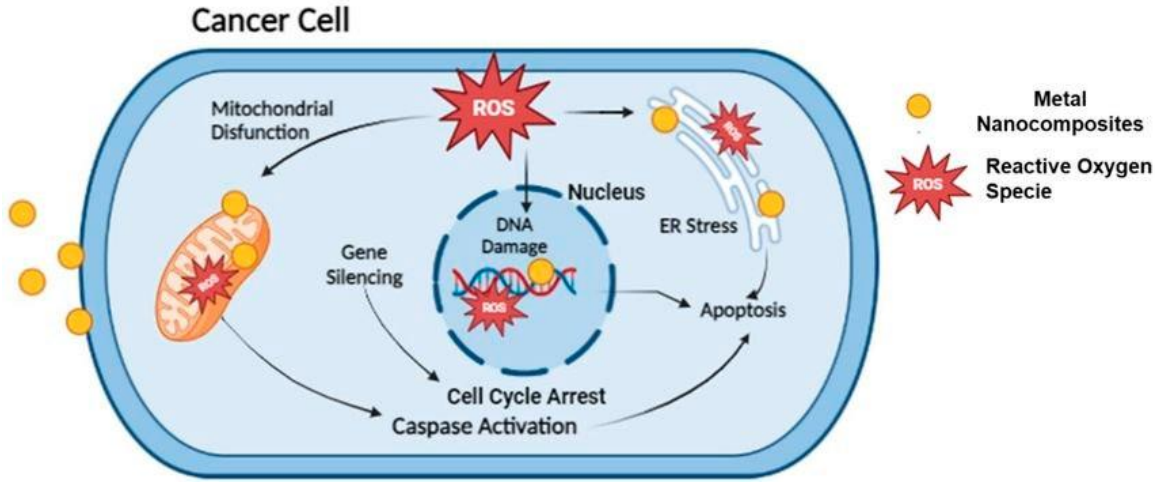

Figure 6:Anticancer Mechanisms of Ag/ZnO Nanoparticles Multiple Pathways of Action.(Aisha Rafique *et al*., 2024)

8.2.Antibacterial Activity of Ag-ZnO Nanocomposites

The hybrid zinc oxide/silver nanoparticles (ZnO/Ag) operate through three main integrated mechanisms that work in perfect harmony to eliminate antibiotic-resistant bacteria and biofilms in particular. The first mechanism is the production of reactive oxygen species (ROS). Upon exposure to light, zinc oxide nanoparticles absorb light energy, leading to the generation of electron-hole pairs. Here, silver plays a crucial role by preventing the recombination of these pairs, thereby extending their reactive lifespan and allowing them to form highly toxic free radicals such as hydrogen peroxide and hydroxyl radicals, which destroy bacterial DNA, proteins, and the cell membrane. The second mechanism is the release of toxic ions, where silver ions (Ag^{+}) and zinc ions (Zn^{2+}) are released from the nanoparticles. Silver ions bind to thiol groups (-SH) in bacterial proteins and disrupt vital enzyme functions, while also adhering to DNA to prevent its replication. Meanwhile, zinc ions disrupt essential metabolic processes. The third mechanism is direct contact and mechanical disruption. These nanoparticles are characterized by a rough surface containing sharp edges due to their crystalline structure. Upon contact with the bacterial cell wall, especially in Gram-negative bacteria, these sharp edges tear and distort the membrane, leading to leakage of cellular contents and bacterial death. What distinguishes these nanoparticles is the synergistic effect, where combining silver with zinc oxide produces far greater efficacy than simply summing the individual effects of each material, allowing the use of lower doses of materials while achieving more efficient antimicrobial results.(Fatima Al Hosani *et al*., 19 Mai 2025)(Elizabeth MaKauki,*et al*.,10 mars 2025).

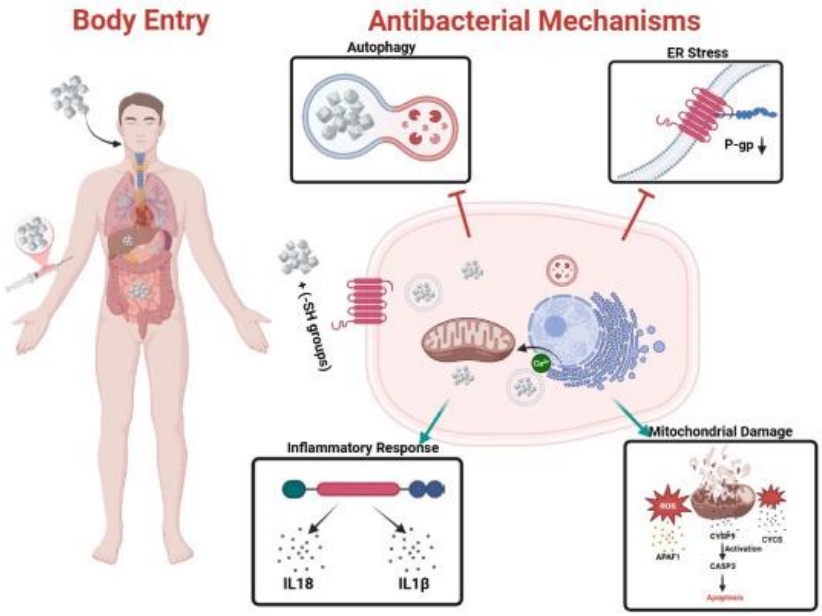

Figure 7: Nanoparticles Body Entry and Antibacterial Mechanisms .(Ibtissam Laib *et al*., 2025).

8.3. Anti-inflammatory Activity

The anti-inflammatory mechanism of zinc oxide nanoparticles (ZnO NPs) primarily relies on inhibiting the NF-κB pathway by inducing the expression of the inhibitory protein A20, which leads to decreased production of pro-inflammatory cytokines such as TNF-α, IL-1β, and IL-6, in addition to their ability to scavenge reactive oxygen species (ROS) with enzyme-like antioxidant activity as demonstrated by DPPH assays (Abdelbaky *et al*., 2022;Kim *et al*., 2015), along with additional inhibition of cyclooxygenase-2 (COX-2) thereby reducing prostaglandin synthesis (Nayal *et al*., 2024). Meanwhile, silver nanoparticles (Ag NPs) act through a complementary mechanism focused on reprogramming immune cells by inducing macrophage polarization from the pro-inflammatory M1 phenotype to the anti-inflammatory M2 phenotype responsible for tissue repair (Chen *et al*., 2020.You *et al*., 2017), in addition to inhibiting the PI3K/Akt pathway and activating autophagy to reduce oxidative stress, while enhancing wound healing through fibroblast stimulation and collagen synthesis (You *et al*., 2017). Both nanoparticle types share enhanced efficacy through their nanosize property., which increases the surface-to-volume ratio, and the release of active ions (Zn^{2+} and Ag^{+}) that directly interfere with intracellular inflammatory signaling pathways (Hussien *et al*., 2025,Lopez-Miranda *et al*., 2023).

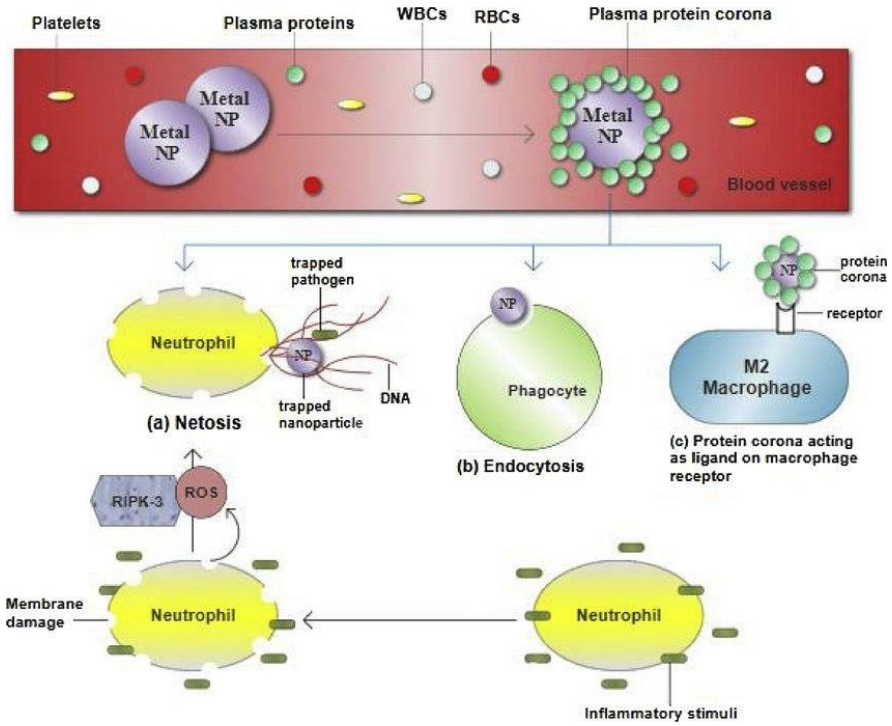

Figure 8: Anti-inflammatory mechanism adopted by nanoparticles. (Agarwal *et al*., 2019).

8.4.Wound Healing Activity

The wound healing activity of silver-zinc oxide nanocomposites (Ag-ZnO) relies on integrated mechanisms that begin with the sustained release of Ag^{+} and Zn^{2+} ions from the nanocomposite matrix upon contact with wound exudate (Rafique *et al*., 2024), where silver ions exert a broad-spectrum bactericidal effect by disrupting the bacterial cell wall, inhibiting respiratory enzymes, and binding to bacterial DNA, while zinc oxide complements this action by generating reactive oxygen species (ROS) and releasing Zn^{2+} ions essential for over 300 metalloenzymes involved in cell division and immunity. The formation of a heterojunction at the Ag-ZnO interface creates a synergistic "dual-channel" effect that eliminates multidrug-resistant bacteria such as MRSA without inducing resistance (Lu *et al*., 2017. Vadhyadevi *et al*., 2026). At the anti-inflammatory level, these nanocomposites inhibit the NF-κB pathway, thereby reducing the secretion of the pro-inflammatory cytokines TNF-α, IL-1β, and IL-6 (Rafique *et al*., 2024), while ZnO exhibits antioxidant activity (up to 86% DPPH scavenging efficiency) that reduces oxidative stress and protects granulation tissue (Kantipudi *et al*., 2018). At the cellular level, Zn^{2+} stimulates fibroblast migration and proliferation, increases the synthesis of collagen types I and III, and enhances extracellular matrix deposition (Ramachandran *et al*., 2024). Furthermore, these nanoparticles upregulate the expression of

vascular endothelial growth factor (VEGF) and CD31 antigen, thereby promoting angiogenesis and improving blood perfusion (Chen *et al*., 2020). When incorporated into advanced dressings such as hydrogels and electrospun nanofibers, studies on diabetic rat models have shown that an Ag/ZnO hydrogel achieves wound closure exceeding 90% within 10–14 days, with complete re-epithelialization, well-organized collagen deposition, and hair follicle regeneration (Rafique *et al*., 2024), confirming that these nanocomposites offer a promising therapeutic approach combining antimicrobial, anti-inflammatory, and tissue-regenerative effects within a single system.

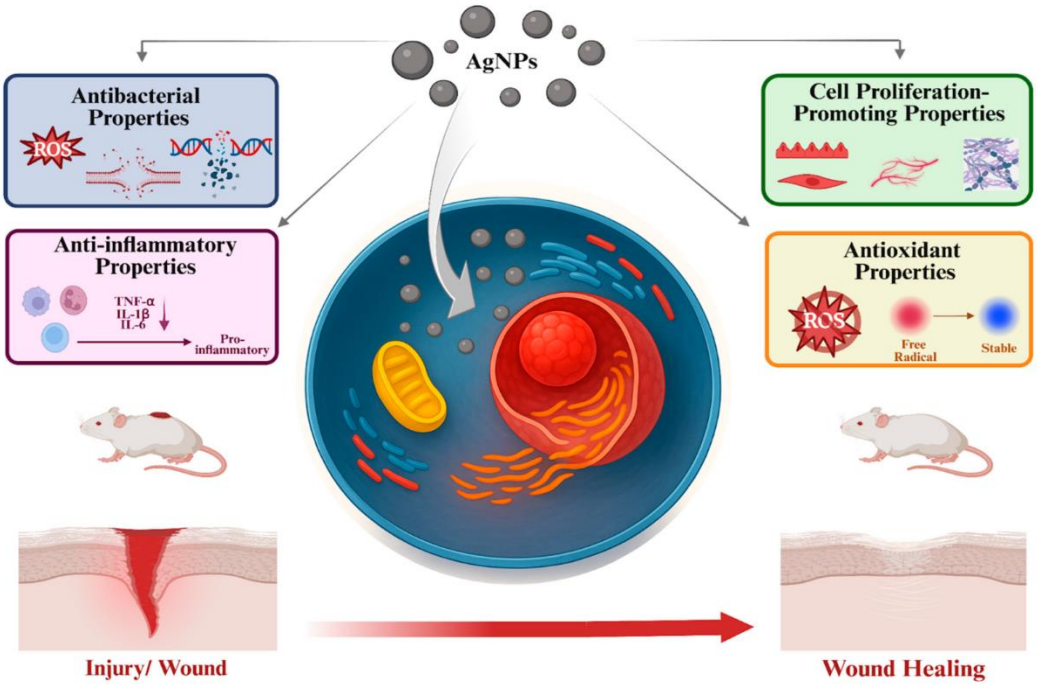

Figure 9: Multifunctional Biological Activities of Silver Nanoparticles (AgNPs) in Wound Healing (Melis Kaya *et al*., 2025).

Second part :

CHAPTER I:

Materials and Methods

1.Materials

1.1Plant material

The *C.sativus Peels*(*Cucumis sativus* var.spp.) were collected during the fruiting period in October 2025 from the southeastern region of Algeria, specifically the El oued Malah area in El Oued (33°40′54.86"N6°54'33.23"E). The plant species was identified by professor Chouikh Atef (Faculty of Natural and Life Sciences, University of El Oued). To remove dust and other foreign particles, the peels were cleaned under running tap water. They were then dried, ground,and stored for subsequent use.

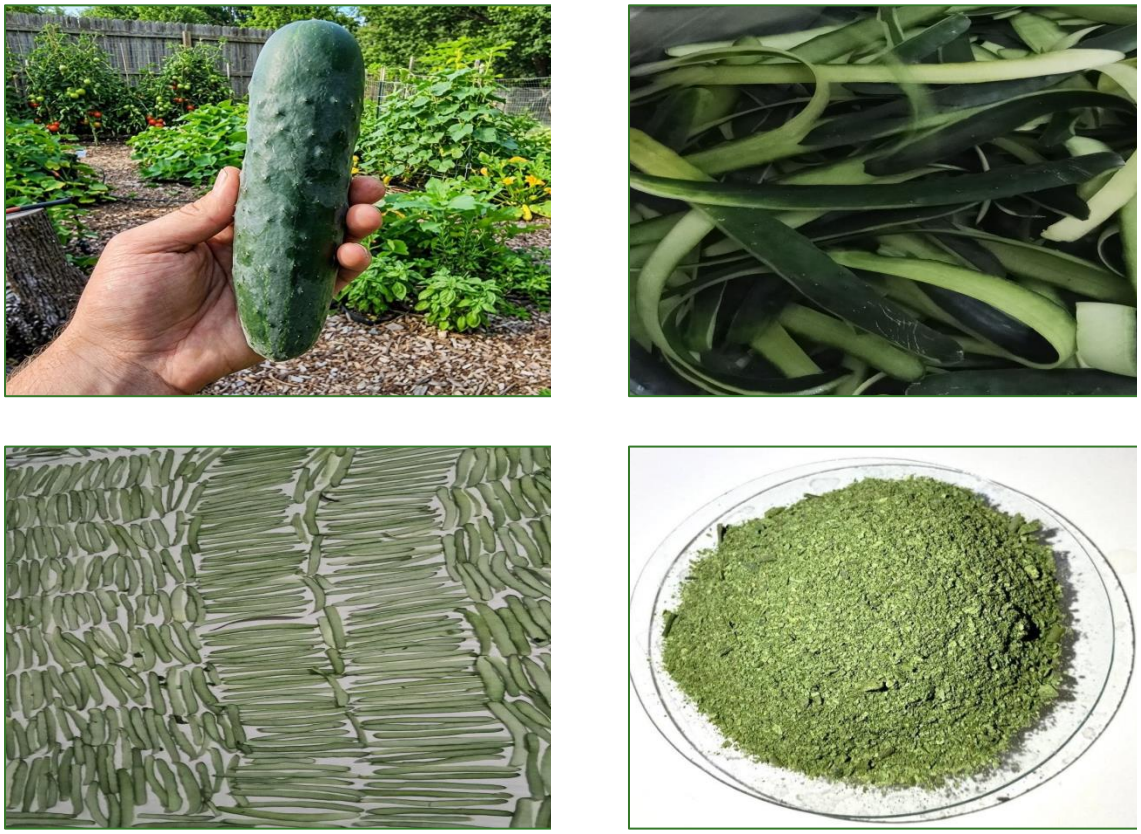

Figure 10: *C.sativus* Peels (Original photo)

1.2.Animals materials

A total of 25 adult albino rats (25 females), weighing Approximately 177.17±11.04, were obtained from the animal house of the pasteur institue, Algeria. They were housed and maintained in the animal facility of the molecular and cellular Biology Department, Faculty of Natural and Life Sciences, University of El-Oued, Algeria. The animals were acclimatized for 2 weeks under standardized laboratory condition, including a photoperiod of 12 hours light/12 hours dark, a relative humidity of 64 ± 2%, and a room temperature of 19 ± 1° C. Standard rat

feed (Southon *et al*., 198) and tap water were provided ad libitum throughout the experimental period. All care and handling procedures for the rats adhered to the recommended practices of the local ethics committe.

1.3.Bacterial Strains

The antibacterial activity of the samples was evaluated on three bacterial strains from the Pasteur Institute laboratory in Algeria,one Gram-positive (BC: *Bacillus subtilis* ATCC 25973;SA) and two Gram-negative (EC: *Escherichia coli* ATCC 25922; KP: *Klebsiella pneumoniae* ATCC 13883).

1.4Chemicals and reagents

The chemicals used are ferric chloride ($FeCl_3$, ≥ 99%),ammonia (NH_3, ≥ 99%), sulphuric acid (H_2SO_4,98%),folin ciocalteu (analytical grade),sodium carbonate (Na_2CO_3, ≥ 99%), Galic acid ($C_7H_6O_5$,≥ 98%), aluminium chloride ($AlCl_3$,≥ 98%), Quercetin ($C_{15}H_{10}O_7$, ≥ 95%), Ethanol (C_2H_6O, ≥ 96%), vanilin ($C_2H_8O_3$, ≥ 98%), catechin ($C_{15}H_{14}O_6$, ≥ 95%), dpph ($C_{18}H_{12}N_5O_6$, ≥ 95%), Potassium ferricyanide(K_3 [Fe (CN)$_6$], ≥ 99%), trichloroacetic acid ($C_2HCl_3O_2$, ≥ 99%), phosphat buffer solution (PBS, NaH_2PO_4/Na_2HPO_4 /NaCl/KCl, ≥ 99%), ammonium molybdate($(NH_4)_6$ $Mo_7O_{24}.4H_2O$,≥ 99%), sodium hydroxide (NaOH, ≥ 98-99%), Sodium Dodecyl Sulfate ($C_{12}H_{25}SO_4Na$,≥ 99%), Silver nitrate ($AgNo_3$,≥ 99 %), Zinc (ZnO, ≥ 99%), Methanol (CM_4O,≥ 99.99).

2.Methods

2.1.Phytochemical analysis of *C.sativus Peels*

2.1.1.Extraction of *C.sativus Peels* Aqueous extract

Ten grams (10 g) of dried *C.sativus Peels* powder were mixed with 100 mL of distilled water to prepare the aqueous extract. The mixture was macerated for 24 hours at room temperaturere with occasional shaking. After maceration, the extract was filtred through watman filter paper and then contrated using a rotary evaporator (TUVE). The resulting extract was weighed, transferred into glass containers, and stored at room temperature until further analysis.(Murgan and Parimelazhagan., 2014)

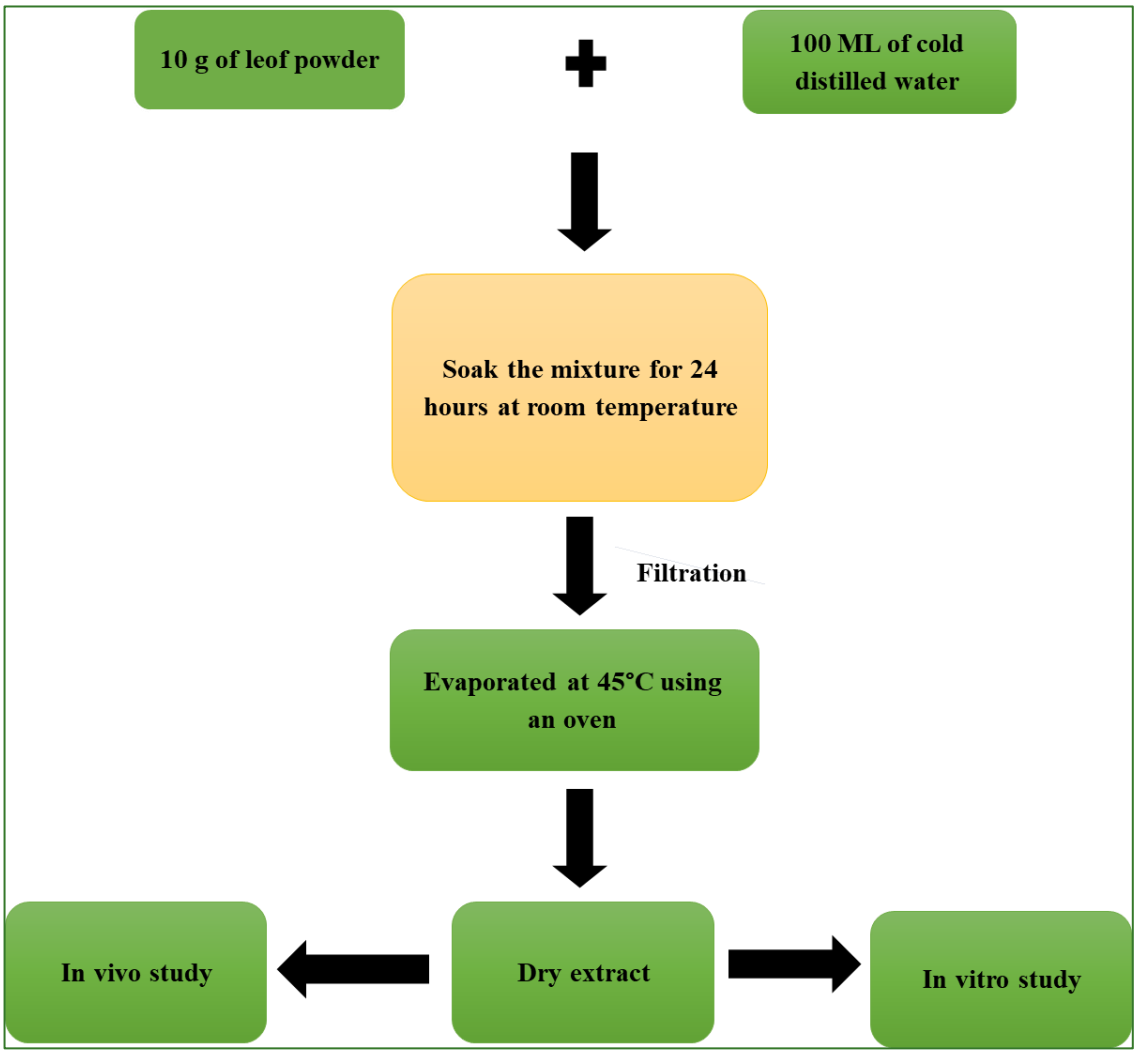

Figure 11: Preparation of Dry Leaf Extract Using Cold Aqueous Extraction Method.

2.1.2.Phytochemical Screening

The active constituents present in the extract of *C.sativus Peels* were identified and detected by performing the following chemical tests :

2.1.2.1.Polyphenols

Two milliliters of the extract were treated with a few drops of 2% (w/v) $FeCl_3$ Solution. The appeance of a greenish or blackish-blue color indicates the presence of polyphenol derivatives.(Sankhalkar and Vernekar., 2016).

2.1.2.2.Flavonoids

Five milliliters of the extract to be tested were added to a test tube containing 5 mL of dilute ammonia and 1 ML of H_2SO_4The presence of flavonoids is demonstrated by the development of a yellow color.(Ibtissam *et al*., 2021).

2.1.2.3.Tannins

Five milliliters of the extract of *C.sativus Peels* were combined in a test tube with 1 ML of a 2% aqueous ferric chloride solution ($FeCl_3$). The development of a greenish or bluish-blackish hue indicates the presence of tannins.(Evans., 2009).

2.1.2.4.Saponins

In a test tube,10 ml of the aqueous *C.sativus Peels* extract was placed. The tube was vigrously saken for 15 minutes.The formation of a persistent foam layer more than 1 cm in height indicated the presence of saponin.(LAIB Ibtissam., 2023)

2.1.3.Quantification of phytochemicals compounds

2.1.3.1.Estimation of total phenolics

The total phenolic content was determined using the Folin-ciocalteu reagent, 0.2mL of the aqueous extract of *C.sativus Peels* was added. After 4 minutes, 800 µl of saturated sodium carbonate solution (75 g/L) was introduced. Following 2 hours of incubation at room temperature, the absorbance was measured at 765 nm. To ensure reproducibility, the tests were performed in triplicate (Slinkard and Singleton., 1977). The total phenolic content was then calculated from the linear calibration aquatoion of gallic acid (used as standard) and expressed as milligrams of gallic acid aquivalents per gram of extract.

2.1.3.2.Estimation of total flavonoids

The aluminum chloride ($AlCl_3$) colorimetric method was employed to determine the total flavonoid content of the *C.sativus Peels* extract as follows : 1mL of the $AlCl_3$ Solution was mixed with 1mL of the sample and separately with 1mL of the standard. After 30 minutes, the absorbance was measured at 430 nm against a prepared reagent blank. A linear calibration equation using quercetin as the standard was utilized to quantify the results. The total flavonoid content was expressed as milligrams of quercetin per gram of exteact .(LAIB Ibtissam., 2023).

2.1.3.3.Estimation of condensed tannin.

The level of condensed tannin in the extract of *C.sativus Peels* was determined spectrophotometrically according to the method described by(Broadhurst and Jones., 1978).

Catechin was used to prepare the calibration curve. The sample was pipetted into an aluminum foil-wrapped tube, mixed with 3.0 mL of freshly prepared vanillin reagent (4% w/v vanillin in methanol), and thoroughly comboined. Then, 1.5 mL of concentrated hydrochloric

acid was added. After 15 minutes at 20 ± 2 °C, the absorbance of the reaction mixture was measured against water at 500 nm.

2.1.3.4.LC-MS/MS analysis of secondary metabolites

The secondary metabolites in the aqueous extract of *C.sativus Peels* were profiled using UPLC-ESI-MS/MS (Shimadzu 8040) operated in Mulyiple Reaction Monitoring (MRM) mode for high selectivitiy and sensitivity. The system was equipped with a binary pump (Nexera XR LC-20AD).

Electrospray ionization (ESI) conditios were set as follows:

Collision dynode-6.00 kV, desolvation line temperature 250°C, nebulizing gas flow 3.0 L/min, heating block temperature 400°C, and drying gas flow 10 L/min. Chromatographic separation was performed on a ResteK Ultra C18 column (3 µm, 150 x 2.1 mm) using 0.1% formica cid in methanol (solvent B) at a flow rate of 0.3 ml/min with an injection volume of 5 µL. The gradient elution program started at 98% A (0-0.2 min), decreased to 25% A (10-15 min). Compounid identification was achieved by comparing MRM transitions, retention time (±0.1 min), and peak areas with an internal database of 55 authenticated standards. The analysis was performed qualitatively.

2.2.Sample preparation (Green Synthesis of Ag-Doped ZnO Nanostructures)

Ag-doped zinc oxid (ZnO) nanostructure were synthesized via a sustainable green synthesis approach,utilizing aqueous *C.sativus Peels* extract (*Cucumis sativus*) as both a primary reducing and stabilizing agent. The experimental procedure commenced with the dissolution of 0.5 M zinc acetate in 100 mL of distilled waterunder magnetic stirring for 30 minutes at room temperature, followed by the incorporatio 0.01M .(Merga Hunde Gonfa and Asnake Lealem Birhanu,. 2024).

2.2.1.Characterization of Sliver- doped Zinc

Silver-doped Zinc nanoparticles were charactized using multiple complementary techniques, including UV-Vis spectroscopy, Fourier transform infrared spectroscopy (FT-IR),X-ray diffraction (XRD), scanning electron microscopy (SEM), and energy dispersive X-ray spectroscopy (EDX).

2.2.1.1.UV-Vis spectrophotometer

The optical properties of the Ag-dopes ZnO were determined using a UV-Vis spectrophotometrer (Shimadzu UV-1800,Japan). Absorption spectra were recorded over the wavelength range of 200-800 nm.

2.2.1.2.X-ray diffraction (XRD)

The crystallines structure of the Ag-doped ZnO was investigated by X-ray power diffraction (PROTO AXRD Benchtop) employing CuKa radiation (30 KV,20 mA) with a wavelength of 0.15281 nm and a scanning speed of 0.05°. Diffraction patterns were collected in the 2 Θ range of 20-80°. The average crystallite size was calculated using the Scherrer equation (Equation 3) by selecting the peak with the highest intensity:

$$\mathbf{D}=\frac{K\lambda}{\beta.\theta}$$

Wher D is the crystallite size, K is the chape factor (0.9), λ is the X-ray wavelength (0.154281 nm,CuKα), β is the full width at half maximum (FWHM), and Θ is the Bragg diffraction angle.

2.2.1.3.Scanning electron microscopy (SEM) and Energy dispersive spectroscopy (EDX)

Scanning electron microscopy (SEM) was used to visualize the surface morphology of the Ag-doped ZnO by directing a focused electron beam of a few nanometers in diameter onto the sample. This technique provides high-magnification images that reveal detailed morphological features. The particle size and shape were determined using a phenom proDesktop scanning electron microscope equipped with an optical magnification range of 20-134x, an electron magnification range of 160-150.000x, and a maximum digital zoom of 12x. The instrument operated at acceleration voltages of 5, 10, and 15 kV and was fitted with a backscattered electron detector (BSD) and an energy dispersive X-ray spectrometer (EDX) with a nominal resolution of 6 nm or less. A temperature-controlled sample holder maintained the analysis temperature between-20°C and 50°C.

2.3.*In Vitro Activity of the aqueous extract of C.sativus Peels ,Silver*

2.3.1.Antioxidant activity

2.3.1.1.DPPH free-radical scavenging activity (DPPH).

One milliliter of the DPPH. Solution was mixed with 1mL of each aqueous extract of cucumber peels (or ascorbic acid as a control). To complete the reaction, the mixture was stirred briefly and then incubated at room temperature for 30 minutes in the dark. The

absorbance of the reaction medium was measured at 517 nm.The percent inhibition (Pl) was calculated using the following equation (Mansouri *et al*., 2005).

$$\textbf{PI (\%)} = \frac{(\textbf{Abs controle} - \textbf{Abs sample})}{\textbf{Abs controle}} \times 100$$

Where Abs-control is the absorbance of control (containing all reagents except the sample) and Abs-sample is the absorbance of the sample.(Gulcin et Alwasel., 2023).

2.3.1.2.Reducing Power Assay (RP)

The reduicing power of the *C.sativus Peels* aqueous extract and the Ag-doped ZnO nanoparticles was determined according to Oyaizu's method. The samples were combined with phosphate buffer (2.5 mL, 0.2 M,pH 6.6) and 1% potassium ferricyanide solution (2.5 ml, $k_3[Fe(CN)_6]$) at various concentrations (mg/mL) in distilled water. After the addition of trichloroacetic acid aliquots (2.5 ml, 10% aqueous solution), the mixture was incubated at 50°C for 20 minutes, followed by centrifugation at 3000 rpm for 10 minutes. The supernatant (2.5 ml) was then mixed with freshly prepared $FeCl_3$ solution (0.5 ml, 0.1%), and the absorbance was measured at 700 nm. Ascorbic acid was used as a positive control. (Oraiza., 1986).

2.3.1.3.Phosphomolybdate assay (Total Antioxidant Capacity)

This assay is based on the capacity of the plant extract and Ag-doped ZnO nanoparticles to reduce Mo (VI) to Mo (V) and subsequently form a green phosphate/Mo (V) complex at acidic PH. An aliquot of 0.3 mL of *C.sativus Peels* extract and Ag-ZnO nanoparticles suspension was mixed with 3 mL of reagent solution (0.6 M sulfuric acid, 28 mM sodium phosphate, and 4Mm ammonium molybdate).

The reaction mixture was incubated in tubes at 95°C for 90 minutes. Afer cooling to room temperature, the absorbance of the solution was measured at 695 nm using a spectrophotometer against a blank. Distilled water (0.3 mL) was used in place of the sample as a control. (Islam *et al.,* 2013). A standard ascorbic acid calibration curve was employed to estimation the ascorbic acid equivalents. The experiment was parformed in triplicate, and the results were expressed as milligrams of ascorbic acid equivalents per gram of extract or nanoparticles.

2.3.2Hemolytic activity

The helytic activity was evaluated according to the method described by vinjamuri *et al*., (2015). Five milliliters of blood were centrifuged at 1000 rmp for 10 minutes at 40°C in tubes containing 5.4 mg of EDTA to prevent coagulation. The assay was performed on washed erythrocytes that had been maintained at 40°C for 6 hours. One hundred microliters of the test samples (crude aqueous extract of *C.sativus Peels*, Ag-doped ZnO nanoparticles) were mixed with 50 µL of the erythrocyte suspension prepared in ten different dilutions. Positive and negative controls consisted of 100 µL of 1x PBS and 100 µL of 1% SDS, respectively. The mixtures were then incubated in a water bath at 37°C for 60 minutes. Subsequently (Vinjamuri *et al*., 2015),850 µL of phosphate-buffered saline (XPB) were added to bring the final volume to 1 ml. After centrifugation at 300 rpm for 3 minutes, the hemoglobin concentration in the supernatan t was determined spectrophotometrically at 540 nm.

The percentage of hemolysis inhibition was calculated using the following formula (Equation 6):

$$\textbf{\% Hemolysis Inhibition} = 100 - \left(\frac{O\ Dsample}{O\ Dcontrol}\right) \times 100$$

2.3.3.Anti-inflammatory activity.

The egg albumin denaturation inhibition method was employed to evaluate the anti-inflammatory potontial of the crude aqueous extract of *C.sativus Peels*, Ag-doped ZnO nanoparticles, The reaction mixture (5 ml) consisted of 200 µL of fresh hen´s egg albumin, 2,8 ml of phsphate buffer (PH 6,4), and 2 ml of the test sample at various concentrations, Diclofenac sodium served as the standard drug, while 2 ml of distilled water was used instead of the extract or drug to prepar the control. After a 15-minute incubation period at 37°C in a water bath, the mixtures were heated for 5 minutes at 70°C. Following cooling, the absorbance was measured at 660 nm using a UV-visible spectrophotometer, with the buffer acting as the blank.(Dharmadeva *et al*., 2018).

The percentag inhibition of egg albumin denaturation was calculated using the following equation:

$$\textbf{Inhibition percentage} = \frac{Acontrol - Asample}{Acontrol} \times 100$$

2.3.4Antibacterial activity assays

As previously mentioned, the agar diffusion method was utilized to determine the antibacterial activity of the tested materials. Prior to the assy, bacterial strains were cultured on nutrient agar for 24 hours at 37°C to reach the stationnary growth phase. Abacterial suspension (10^6 colony-forming units per mL) was uniformly spread onto Mueller-Hinton agar plates using sterile swabs. Sterile discs (6 nm in diametre) were then impregnated with 10 µL of the various *C.sativus Peels* extracts, Ag-doped ZnO nanoparticles, or fraction (all dissolved in 5% DMSO, v/v) at different concentrations. Amoxicillin (10 µg/mL) and cephalexin (30 µg/mL) were used as positive controls, while 5% DMSO (v/v) served as the negative control. The plates were incubated at 37°C for 24 hours (Goanar, Tafesse, et Fereja., 2024).

2.4.*In vivo* activity of aqueous extract of *C.sativus Peel* and Ag/ZnO

2.4.1. Formulation of Burn-Healing Cream

Burn-healing creams were prepared using a Vaseline® base containing aqueous *C.sativus Peels* extract and Ag/ZnO nanoparticules at concentration of 10%, 0.1% respectively (w/w). The selection of, 10%,0.1% (w/w) *C.sativus Peels* extract and Ag/ZnO concentration was deliberate and grounded in established experimental practice. This concentration range aligns with previously published studies investigating plant-based topical formulations in burn and excisional wound models (E.Nasiri *et al*., 2017). The extract was slowly blended into the melted base in a water bath at 45 °C under continuous stirring until a homogeneous mixture was obtained. The creams were then cooled to room temperature, transferred into sterile, airtight containers, and stored at 4 °C for subsequent evaluation. MEBO® cream was used as the reference standard for comparison of wound-healing efficacy (K.Segueni *et al*., 2025).

2.4.2. Physicochemical and Dermal Safety Evaluation

The pH of cream formulations was determined by dispersing 1 g of cream in 10 mL distilled water, filtering with Whatman No. 4 paper, and measuring at 20 °C using a calibrated pH meter (HANNA-HI 8424) in triplicate to ensure accuracy.

Stability was assessed by centrifuging formulations at 3000 rpm for 30 min at room temperature, with visual inspection for phase separation, oiling off, or texture changes. Stability was rated 100% (fully stable) to 0% (unstable), with creams maintaining texture, pH, and activity over the evaluation period.

Viscosity was measured using a Brookfield viscometer at 25 °C to ensure suitable topical application, while spreadability was tested by placing 1 g of cream between glass slides and measuring the spread diameter under 100 g for 30 seconds.

Acute dermal safety was evaluated per OECD guideline 402, applying 50 mg of cream to a 4 cm^2 shaved dorsal area of male Wistar rats (150-200g) housed under standard conditions. Rats were observed for 7 days for erythema, edema, or toxicity, with procedures approved by the University of El Oued's IAEC .(A.D.Ankomah *et al*., 2022).

Acute dermal safety was assessed following OECD guidelines, applying 50 mg of each cream to shaved dorsal skin of male Wistar rats under standard conditions with food and water access. Rats were monitored for 7 days for irritation, erythema, edema, or systemic toxicity, approved by the University of El Oued's IAEC.

2. 5.Wound healing evaluation of the formulated burn healing cream

Adult Wistar albino rats were acclimatized for two weeks under standard laboratory conditions before experimentation. The animals were randomly assigned into five groups (n = 5 per group) using a computer-generated random number sequence (SPSS software, version 26.0).

Blinding and Measurement Procedures:

- **Histological analysis**: Tissue sections were coded, and scoring of re-epithelialization, collagen deposition, and inflammatory infiltration was performed by an independent technician blinded to treatment allocation.
- **Hematological analysis**: Blood samples were anonymized prior to analysis, and all measurements were performed using automated analyzers to eliminate operator influence.
- **Wound area measurements**: Standardized digital imaging and software-assisted quantification were employed.

All treatments were topically applied once daily, starting on the second day after burn induction, and continued for 21 days, as summarized in Table 1.

Table 2: Experimental Groups of Wistar Albino Rats and Corresponding Topical Treatments for Burn Wound Healing

Group	Treatment Description
I	Burned, untreated control
II	Burned rats treated with cream base only
III	Burned rats treated with *C.sativus Peels* extract cream (10%)
V	Burned rats treated with Ag-doped ZnO nanoparticles cream (0.1%)
VI	Burned rats treated with MEBO® medical cream

Burn wounds were induced following Tavares Pereira *et al*., (2012)(Tavares Pereira *et al*., 2012), using xylazine-anesthetized rats with shaved, 70% ethanol-disinfected dorsal skin. A preheated 1 cm metal cylinder was applied for 15 s to create standardized burns, and 50 mg *C.sativus Peels* extract creams were applied daily at 10:00 a.m. until closure, with healing tracked via photographs.

At study's end, rats were euthanized with ketamine and xylazine via decapitation. Blood was collected in EDTA tubes for hematological analysis, and skin tissues were excised for histopathology at BABDA, University of El Oued, adhering to ethical guidelines approved by the Institutional Ethics Committee.

Wound healing was monitored by photographing lesions and measuring length and width every two days over 21 days, with the percentage of wound contraction calculated using a standard formula (Subramanian *et al*., 2023):

$$\textbf{Wound contraction (\%)} = \left[\frac{\textbf{wound Area on Day 0} - \textbf{wound Area on Day n}}{\textbf{wound Area on Day 0}}\right] \times \mathbf{100} \quad (6)$$

Figur 12: Expermental Desing for Evaluating the Efficacy of Different Treatments on Burn Wound Healing in Female Albino Wistar Rats.

2.6.Samples Preparation

2.6.1. Hematological Parameters

Hematological parameters, including RBC count, Hb concentration, HCT, platelet count, and WBC count, were evaluated using an automated hematology analyzer (Medonic, Boule Diagnostics AB, Sweden).

2.6.2.Histopathological Evaluation

Following euthanasia , the dorsal burn area of each animal was carefully shaved using a sterile scalpel to reduce the rick of contamination. A skin biopsy was then obtained from the center of the burned region using a fresh, sharp surgical blade. The excised tissue samples

were immediately immersed in 10% neutral-buffered formalin for fixation to preserve cellular architecture and prevent autolysis. The samples were left in the fixative overnight at room temperature prior to further processing. The fixed tissues were subsequently embedded in paraffin blocks and sectioned into thin slices of 4-6 µm thickness using a Thermo Scientific Microm HM 325 rotary microtome. The sections were stained with hematoxylin and eosin (H&E), the standard staining technique for general morfological evaluation. For each animal, three independent slides were prepared and examined under a light microscope to evaluate histological changes in the skin, including epidermal thickness, dermal organization, inflammatory cell infiltration, and any other structural or cellular abnormalities.

2.7. Statistical Analysis

Statistical analysis was performed using SPSS software (Version 26.0). Data were expressed as mean ± standard error of the mean (SEM). Prior to analysis, normality and homogeneity of variance were assessed to confirm the suitability of parametric tests. One-way analysis of variance (ANOVA) was applied to evaluate significant differences among groups. When significant differences were detected, Tukey's Honestly Significant Difference (HSD) post hoc test was used for multiple pairwise comparisons. a p-value of less than 0.05 ($p < 0.05$) was considered statistically significant.

CONCLUSION

CONCLUSION

In conclusion, the present study successfully demonstrates the remarkable therapeutic potential of *Cucumis sativus* (cucumber) peels and the green-synthesized Ag/ZnO nanocomposite derived from them in accelerating burn wound healing. Through a comprehensive and integrated approach encompassing phytochemical profiling, advanced nanomaterial characterization, in vitro bioassays, and in vivo experimental validation, this research provides robust scientific evidence that the combination of these natural resources with green nanotechnology yields a powerful, multifunctional, and sustainable therapeutic agent.

Phytochemical analysis using LC-MS/MS revealed a rich and diverse profile of bioactive secondary metabolites in C. sativus peels, overwhelmingly dominated by L-proline, alongside significant amounts of potent polyphenols (such as myricetin and resveratrol), phenolic acids (sinapic and ferulic acids), and organic acids. These phytoconstituents played a crucial dual role: acting as highly efficient reducing and capping agents during the green synthesis process, while also contributing directly to the biological activities of the final material.

The green synthesis was highly successful, as confirmed by comprehensive characterization. The resulting Ag/ZnO nanocomposite exhibited a highly crystalline biphasic structure with an average crystallite size of 28.97 ± 0.98 nm, characteristic optical properties, strong bio-capping by plant-derived functional groups, and a desirable porous cauliflower-like morphology with high silver content.

In vitro investigations demonstrated that the Ag/ZnO nanocomposite possessed markedly superior antioxidant, anti-inflammatory, and photoprotective activities compared to the crude peel extract, along with excellent biocompatibility. Most notably, in vivo evaluation in a second-degree burn wound model in Wistar rats showed that the 0.1% Ag/ZnO nanocomposite cream dramatically accelerated wound contraction, achieving near-complete closure by days 18–21. It significantly outperformed both the 10% *C. sativus* peels extract cream and the commercial reference MEBO®, with superior re-epithelialization, well-organized collagen deposition, enhanced angiogenesis, and reduced inflammatory response. Hematological and histopathological analyses further confirmed its safety and efficacy in restoring normal physiological parameters.

Overall, this work proudly transforms an abundant and underutilized agricultural waste into a high-value, eco-friendly nanotherapeutic product. It stands as a shining example of how traditional phytotherapy and modern green nanotechnology can be elegantly integrated to

address critical medical challenges. By establishing a sustainable nanotherapeutic platform for advanced burn wound management, this study strongly supports the principles of agricultural waste valorization and circular economy, while highlighting the strategic importance of Algeria's medicinal plant heritage in developing innovative and accessible healthcare solutions.

Future Perspectives

Building upon these encouraging findings, future research will open exciting new horizons, including:

- ✓ Bioguided isolation and purification of the most active phytochemical compounds (especially L-proline and key polyphenols) to better understand their individual contributions.
- ✓ In-depth molecular and cellular mechanistic studies to unravel the precise signaling pathways (TGF-β, VEGF, NF-κB, and MMPs) modulated by the nanocomposite.
- ✓ Development of advanced and smart delivery systems such as bioactive hydrogels, nanofiber mats, and controlled-release dressings to maximize therapeutic efficacy and patient comfort.
- ✓ Preclinical optimization and human clinical trials aimed at translating these promising laboratory results into safe, effective, and commercially viable therapeutic solutions.

Reference

References

A

1.Abd El-Hamid, M. I., et al. (2024). Silver nanoparticles loaded with pomegranate peel extract and hyaluronic acid mediate recovery of cutaneous wounds infected with Candida albicans. Frontiers in Cellular and Infection Microbiology, 14, 1469493.

2.Abdelbaky, A. S., et al. (2022). Green synthesis and characterization of ZnO nanoparticles using Pelargonium odoratissimum leaf extract: Antioxidant, antibacterial and anti-inflammatory activities.

3.Ahmed, S., et al. (2019). A review on plants extract mediated synthesis of silver nanoparticles for antimicrobial applications: A green expertise. Journal of Advanced Research, 7, 17–28.

4.Ahsan, H., et al. (2024). Efficacy of silver oxide nanoparticles against multidrug-resistant Pseudomonas aeruginosa and methicillin-resistant Staphylococcus aureus in burn wound infections. Asian Journal of Agriculture and Biology.

5.Al Shammari A,A.Science: Nanotechnology and Nanoscience.

6.Al-Allaf, F. A., & Albaker, A. M. (2023). Green synthesis of ZnO nanoparticles and their biomedical applications in wound healing. Materials Today Communications, 35, 105000.

7.Albaugh, V. L., Mukherjee, K., & Barbul, A. (2017). Proline metabolism and its role in tissue repair and regeneration. Journal of Surgical Research, 219, 1–10.2022).

8.Albaugh, V. L., Mukherjee, K., & Barbul, A. (2017). Proline precursors and collagen synthesis: Biochemical challenges of nutrient supplementation and wound healing. Journal of Nutrition, 147(11), 2011–2017.

9.Alharbi, F. N., Abaker, Z. M., & Makawi, S. Z. (2023). Phytochemical substances–mediated synthesis of zinc oxide nanoparticles (ZnO NPs). Inorganics, 11, 328.

10.Alharthi, F. A., et al. (2023). Biosynthesis of Ag-doped ZnO nanoparticles using Cucumis sativus extract: FTIR and XRD studies. Ceramics International, 49(12), 20456–20465.

11.Alharthi, F. A., et al. (2023). Biosynthesis of Ag/ZnO nanocomposites using Cucumis sativus extract: Optical, structural and morphological studies. Ceramics International.

12.Ali, Akbar, et al. (2019). Green Synthesis of Metal, Metal Oxide Nanoparticles, and Their Various Applications.

13.Alvarez-Suarez, J. M., Giampieri, F., & Battino, M. (2012). Honey as a source of dietary antioxidants: Structures, bioavailability and evidence of protective effects against human chronic diseases. Current Medicinal Chemistry, 20(5), 621–638.

14.Al-Zubaidi, S. H., Al-Rubaye, A. F., & Abdul-Hussein, M. A. (2019). Evaluation of Aloe vera gel for burn healing and antioxidant activity. Journal of Pharmaceutical Sciences and Research, 11, 344–349.

15.Ani, V., Varadarajan, S., & Nair, M. (2023). Flavonoids and phenolic acids as anti-inflammatory agents: Mechanisms of action and therapeutic potential. Biomedicine & Pharmacotherapy, 158, 114–122.

16.Ankomah, A.D., et al. (2022). Evaluation of dermal toxicity and wound healing activity of Cnestis ferruginea Vahl ex DC. Adv. Pharmacol. Pharm. Sci., Article 5268613.

17.Anosike, C. A., Obidoa, O., & Ezeanyika, L. U. S. (2019). Membrane stabilization as a mechanism of the anti-inflammatory activity of plant extracts. Journal of Basic and Clinical Physiology and Pharmacology, 30(2), 1–9.

18.Apak, R., et al. (2016). Antioxidant activity/capacity measurement: Classification, physicochemical principles, mechanisms, and electron transfer (ET)-based assays. Journal of Agricultural and Food Chemistry, 64, 997–1027.

19.Apak, R., et al. (2019). Antioxidant activity/capacity measurement methods for food and biological samples. Journal of Agricultural and Food Chemistry, 67, 918–932.

20.Aquino, P. E. A., et al. (2019). The wound healing property of N-methyl-(2S,4R)-trans-4-hydroxy-L-proline from Sideroxylon obtusifolium is related to its anti-inflammatory and antioxidant actions. Journal of Evidence-Based Integrative Medicine.

21.Arifianto, N., et al. (2024). Antipyretic activity test of cucumber (Cucumis sativus L.) ethanol and methanol extract on male white mice (Mus musculus).

22.Asgary, S., Naderi, G. H., & Askari, N. (2005). Protective effect of flavonoids against red blood cell hemolysis by free radicals. Experimental & Clinical Cardiology, 10(2), 88–90.

23.Augustine, R., et al. (2021). Role of nanoparticles in wound healing. Nanomaterials, 11(11), 2948.

B

24. Baliyan, S., et al. Determination of antioxidants by DPPH radical scavenging activity and quantitative phytochemical analysis of Ficus religiosa.

25. Bayisa, Y. M., et al. (2023). Ecofriendly green synthesis and characterization of silver zinc oxide nanocomposite using Rumex crispus leaf extract. Heliyon, 9(5), e16245.

26. Ben Dania, Jouria, & Ghattas, Jamila. (2024). Green synthesis of nanomaterials from plant sources - Lagenaria siceraria. [Unpublished master's thesis]. University of Kasdi Merbah Ouargla.

27. Benayad, Z., et al. (2014). Phenolic composition, antioxidant and anti-inflammatory activities of extracts from Moroccan Opuntia ficus-indica flowers obtained by different extraction methods. Industrial Crops and Products, 62, 412–420.

28. Beretta, G., et al. (2020). Standardization of antioxidant properties of polyphenols and their role in wound healing. Molecules, 25(5), 1131.

29. Bharathi, D., et al. (2022). Green synthesis and characterization of zinc oxide nanoparticles using plant extract: Antioxidant and anti-inflammatory activities.

30. Burlec, Ana Flavia, et al. (2023). Current Overview of Metal Nanoparticles' Synthesis, Characterization, and Biomedical.

C

31. Carvalho, M. T. B., et al. (2021). Wound healing properties of flavonoids: A systematic review highlighting the mechanisms of action. Phytomedicine, 90, 153636.

32. Chaima, B., et al. (2025). Polyphenolic Profiling and Wound Healing Potential of Hammada scoparia (Pomel) Iljin: Preclinical Evaluation of a Novel Topical Formula. Natural Product Communications, 20(1).

33. Chen, Y., et al. (2020). Improved immunoregulation of ultra-low-dose silver nanoparticle-loaded TiO_2 nanotubes via M2 macrophage polarization by regulating GLUT1 and autophagy.

34. Costa, M. F., et al. (2019). Effects of carvacrol, thymol and essential oils on wound healing: A systematic review. Journal of Pharmacy and Pharmacology, 71(2), 141–155.

35. Cyboran, S., Oszmiański, J., & Kleszczyńska, H. (2012). Interaction between plant polyphenols and the erythrocyte membrane. Cellular & Molecular Biology Letters, 17(1), 77–88.

D

36. Dangana, R. S., et al. (2023). Facile biosynthesis, characterization and biotechnological application of ZnO nanoparticles mediated by plant extract. Artificial Cells, Nanomedicine, and Biotechnology, 51(1), 309–317.

37. Dash, P., Gochhi, M., & Ghosh, G. (2023). Green synthesis of zinc oxide nanoparticles using plant extract and their antibacterial activity. Minerva Biotechnology and Biomolecular Research, 35(2), 81–89.

38. Dhanalakshmi, R., et al. Green synthesis of Ag/ZnO nanocomposites: XRD confirmation of biphasic structure.

39. Dharmadeva, S., et al. (2018). In vitro anti-inflammatory activity of Ficus racemosa L. bark using albumin denaturation method. Ayu, 39(4), 239.

40. Dhawale, S. K., et al. (2025). Studies on Photocatalytic... Ag-embedded ZnO nanocomposites.

41. Do, Q. D., et al. (2020). Effect of extraction solvent on total phenol content and antioxidant activity. Journal of Food and Drug Analysis, 28, 27–36.

E & F

42. Evans, W. C. (2009). Trease and Evans' pharmacognosy (16th ed.). Saunders Elsevier.

43. Faisal, S., et al. (2021). Green synthesis of metal nanoparticles and their biomedical applications. Journal of Nanomaterials, Article ID 6695452.

44. Fakhar Abbas, et al. (2022). Response surface methodology for the extraction of polyphenol contents and HPLC profiling of Cucumis sativus peels.

G

45. Gaikwad, S., et al. (2022). Green synthesis of silver and zinc oxide nanoparticles and their biomedical applications. Biotechnology Reports, 34, e00716.

46. Gehring, W. (2021). Nicotinic acid/niacinamide and the skin. Journal of Cosmetic Dermatology, 20, 167–173.

47. Ghaemi, B., et al. (2018). Intracellular ROS induction by Ag@ZnO core–shell nanoparticles: Frontiers of permanent optically active holes in breast cancer theranostic.

48. Goanar, G., Tafesse, G., & Fereja, W. M. (2024). In vitro antibacterial activity of fruit pulp extracts of Tamarindus indica against Staphylococcus aureus and Klebsiella pneumoniae. BMC Complementary Medicine and Therapies, 24, 127.

49. Goel, T., et al. (2024). Synthesis, characterization of ZnO@PDA@Ag nanocomposite: Mechanistic interaction with BSA, photodegradation activity & in vitro cytotoxicity assay on H1299 lung cancer cell line.

50. Gómez-Zorita, S., et al. (2021). Resveratrol and its anti-inflammatory and antioxidant effects in wound healing. Nutrients, 13(9), 3015.

51. Guevara-Figueroa, T., et al. (2010). Proximate composition, phenolic acids, and flavonoids characterization of commercial and wild nopal (Opuntia spp.). Journal of Food Composition and Analysis, 23(6), 525–532.

52. Gülçin, İ. (2020). Antioxidants and antioxidant methods: An updated overview. Archives of Toxicology, 94, 651–715.

53. Gülçin, İ., & Alwasel, S.H. (2023). "DPPH Radical Scavenging Assay." Scientific Research Publishing, 74.

54. Gunasekaran Vidhyadevi & S. R. Suseem. (2026). Green synthesis of Ag/ZnO nanocomposites from Phyllanthus emblica seed for multifunctional wound healing applications. Scientific Reports, 16.

H

55. Hamdani, S., et al. (2021). Antioxidant activity and phytochemical profile of Opuntia ficus-indica seed extracts from Algeria. African Journal of Modern Agricultural Practices, 8(1), 23–31.

56. Hashemi, B., et al. (2021). Antibacterial and wound healing properties of metal nanoparticles. Materials Science and Engineering C, 118, 111533.

57. Hosny Shimaa, et al. (2025). A Comprehensive Review of Silver Nanoparticles (AgNPs): Synthesis Strategies, Toxicity Concerns, Biomedical Applications, AI-Driven Advancements, Challenges, and Future Perspectives.

58. Hussien, N. A., El-Ansary, A., & El-Sayed, W. M. (2025). Green synthesis of zinc oxide nanoparticles using clove buds extract: Antibacterial, anticancer, and anti-inflammatory activities.

I

59. Ibtissam, L., Samir, D., & Wiam, Z. (2021). Aristolochia longa (Aristolochiaceae) Spice Alleviates Nickel-Induced Oxidative Stress and Biochemical Alterations in Rats. Austin J Pharmacol Ther, 9(6), 1151.

60. Irede, E. L., et al. (2024). Cutting-edge developments in zinc oxide nanoparticles: synthesis and applications for enhanced antimicrobial and UV protection in healthcare solutions. RSC Advances, 14, 20992–21034.

61. Islam, E., et al. (2013). Estimation of total phenol and in vitro antioxidant activity of Albizia procera leaves. BMC research notes, 6(1), 1-7.

J & K

62. Jovanovic, M., Vojinovic Miloradov, M., & Cveticanin, L. (2024). Effect of silver nanoparticles in treating and healing of burn wound. Journal of the Serbian Chemical Society, 89(5), 617–626.

63. Kantipudi, S., et al. (2018). Enhanced wound healing activity of Ag–ZnO composite nanoparticles. Journal of Photochemistry and Photobiology B: Biology, 185, 349–356.

64. Karna, E., et al. (2020). Proline-dependent regulation of collagen metabolism. Cellular and Molecular Life Sciences, 77, 1911–1918.

65. Khaliq, T., Ahmad, S., & Iqbal, Z. (2022). Antioxidant potential of prickly pear peel extract. Food Science & Nutrition, 10, 1500–1508.

66. Khanjari, Z., et al. (2024). Unlocking the therapeutic potential: Green synthesized zinc oxide/silver nanoparticles from Sophora pachycarpa for anticancer activity, gene expression analysis, and antibacterial applications.

67. Kim, D.-O., Jeong, S. W., & Lee, C. Y. (2014). Antioxidant capacity of phenolic phytochemicals from various plant sources. Food Chemistry, 81, 321–326.

68. Kim, M. H., et al. (2015). Zinc oxide nanoparticles suppress LPS-induced NF-κB activation by inducing A20, a negative regulator of NF-κB, in RAW 264.7 macrophages.

69. Kordy, M. G. M., et al. (2022). Green synthesized silver nanoparticles for wound healing applications: A review. Journal of Nanomaterials, Article ID 123456.

70. Kumar, B., et al. (2020). Green synthesis of Ag decorated ZnO nanoparticles using peel extracts: FTIR, XRD and UV-Vis characterization. Materials Today: Proceedings, 26, 123–130. (Materials Science & Engineering C).

71. Kumar, M., et al. (2020). Functional properties and antioxidant activity of plant extracts: A review. Journal of Food Science and Technology, 57, 1–17.

72. Kumar, S., Pandey, A. K., & Singh, P. (2019). Antioxidant activity and free radical scavenging capacity of plant extracts. Biomedicine & Pharmacotherapy, 111, 110–120.

73. Kumar, S., Yadav, A., & Yadav, M. (2020). Evaluation of antioxidant activity of plant peel extracts using DPPH assay. Journal of Food Science and Technology, 57, 287–295.

L

74. LaFoya, B., et al. (2019). Notch signaling and its role in angiogenesis. Advances in Experimental Medicine and Biology, 1131, 131–151.

75. Laib Ibtissam. (2023). Green synthesis and characterization of silver nanoparticles based on Helianthenum lippii L. extract and evaluation of their biological activities. Doctoral Thesis, University of Echahid Hamma Lakhdar - El Oued, Algeria.

76. Lakshmanan, R., & Maulik, N. (2018). Development of next generation cardiovascular therapeutics through bio-assisted nanotechnology. Journal of Biomedical Materials Research Part B, 106(5), 2072-2083.

77. Lansdown, A. B. G. (2007). Zinc in wound healing: Theoretical, experimental, and clinical aspects. Wound Repair and Regeneration, 15(1), 2–16.

78. Lee, H. J., Kim, M. K., & Park, J. Y. (2017). Protective effects of plant-derived antioxidants against UV-induced oxidative damage. Korean Citation Index Journal.

79. Lee, J., Koo, N., & Min, D. B. (2017). Reactive oxygen species, aging, and antioxidant nutraceuticals. Comprehensive Reviews in Food Science and Food Safety.

80. Leopoldini, M., Russo, N., & Toscano, M. (2021). The molecular basis of working mechanism of natural polyphenolic antioxidants. Food Chemistry, 125, 288–306.

81. Lodish, H., et al. (2021). Molecular cell biology (9th ed.). W. H. Freeman and Company.

82. Long An (2015). Cucumis sativus-Cucumber. The Worlde Vegetables.

83. Lopez-Miranda, J. L., et al. (2023). Antibacterial and anti-inflammatory properties of ZnO nanoparticles synthesized by a green method using Sargassum extracts.

84. Lopez-Miranda, J. L., Escribano-Lopez, I., & Tunez, I. (2023). Nanoparticles as modulators of oxidative stress and inflammation in biomedical applications. Antioxidants, 12, 1450.

85. Loretta, B., & Oliviero, M. (2019). Quality by design approach to optimize cladodes soluble fiber processing extraction in Opuntia ficus indica (L.) Miller. J. Food Sci. Technol., 56, 3627-3634.

M

86. Makauki, E., et al. (2023). Facile biosynthesis of Ag–ZnO nanocomposites using Launaea cornuta leaf extract.

87. Makauki, E., et al. (2025). Synergistic antimicrobial mechanisms of silver-doped zinc oxide for water treatment: a systematic review.

88. Mansfeld, B. N., et al. (2017). Transcriptomic and metabolomic analyses of cucumber fruit peels reveal a developmental increase in terpenoid glycosides associated with age-related resistance to Phytophthora capsici.

89. Mansouri, A., et al. (2005). Phenolic profile and antioxidant activity of the Algerian ripe date palm fruit (Phoenix dactylifera). Food Chemistry, 89(3), 411–420.

90. Marslin, G., et al. (2018). Secondary Metabolites in the Green Synthesis of Metallic Nanoparticles. (Frontiers in Plant Science).

91. Merga Hunde Gonfa, & Asnake Lealem Birhanu. (2024). Green synthesis, characterization and antibacterial evaluation of ZnO and Ag-doped ZnO nanoparticles using Ruta chalepensis leaf extract. Green Chemistry Letters and Reviews, 17(1), 2412613.

92. Minh, N. P. (2021). Evaluation of antioxidant capacity of plant extracts using DPPH method. International Journal of Scientific Research in Science and Technology, 8(2), 120–126.

93. Mtavangu, S. G., et al. (2022). In situ facile green synthesis of Ag–ZnO nanocomposites using Tetradenia riparia leaf extract and their photocatalytic activity. Scientific Reports, 12, 12345.

94. Mukherjee, P. K., Venkatesh, P., & Ponnusankar, S. (2013). Ethnopharmacology and therapeutic potential of plant secondary metabolites in inflammation. Journal of Ethnopharmacology, 146, 1–15.

95. Munteanu, I. G., & Apetrei, C. (2021). Analytical methods used in determining antioxidant activity: A review. International Journal of Molecular Sciences, 22(7), 3380.

96. Murugan, R., & Parimelazhagan, T. (2014). Comparative evaluation of different extraction methods for antioxidant and anti-inflammatory properties from Osbeckia parvifolia Arn. – An in vitro approach. Journal of King Saud University – Science, 26(4), 267–275.

N & O

97. Naim, N., et al. (2022). Chemical composition profiling and antifungal activity of saffron petal extract. Molecules, 27(24), 8742.

98. Naim, N., et al. (2022). Flavonoid composition and antibacterial properties of Crocus sativus L. petal extracts. Molecules, 28(1), 186.

99. Nasiri, E., et al. (2017). The effects of Punica granatum flower extract on skin injuries induced by burn in rats. Adv. Pharmacol. Pharm. Sci., Article 3059745.

100. Nasrollahzadeh, Mahmoud, et al. (2019). An Introduction to Nanotechnology.

101. Nayal, R., Mejjo, D., & Abajy, M. Y. (2024). Anti-inflammatory properties and safety of green synthesized zinc oxide nanoparticles: A review.

102. Olszowy, M., & Tomczyk, M. (2020). How to express antioxidant properties of substances properly? Chemical Papers, 74, 615–628.

103. Oraiza, M. (1986). Studies on product of browning reaction prepared from glucosamine. Japanese J Nutr, 44, 307-315.

104. Oulahal, N., & Degraeve, P. (2021). Phenolic-rich plant extracts with antimicrobial activity. Frontiers in Microbiology, 12, 753518.

P & R

105. Pereira, M. T., Barretto, R. O., & Lima, S. M. (2012). Experimental burn model in rats for wound healing studies. Acta Cirúrgica Brasileira, 27(10), 690–695. D. dos Santos Tavares Pereira).

106. Poljšak, N., Kreft, S., & Kočevar Glavač, N. (2020). Vegetable butters and oils in skin wound healing: Scientific evidence for new opportunities in dermatology. Phytotherapy Research, 34(2), 254–269.

107. Prieto, P., Pineda, M., & Aguilar, M. (1999). Spectrophotometric quantitation of antioxidant capacity through the formation of a phosphomolybdenum complex. Analytical Biochemistry, 269(2), 337–341.

108. Primavilla, S., et al. (2022). Antibacterial activity of Crocus sativus L. petals extracts against foodborne pathogenic and spoilage microorganisms. Life, 13(1), 60.

109. Priyadarshini, S., et al. (2020). Antioxidant activity and phytochemical analysis of Cucumis sativus peels.

110. Puntel, R. L., Nogueira, C. W., & Rocha, J. B. T. (2020). Krebs cycle intermediates modulate oxidative stress and antioxidant defenses. Toxicology in Vitro, 24, 307–313.

111. Rafique, A., et al. (2024). Chia seed-mediated fabrication of ZnO/Ag/Ag_2O nanocomposites: Structural, antioxidant, anticancer, and wound healing studies. Frontiers in Chemistry, 12, 1405385.

112. Rajasekar, M., et al. (2024). Recent developments in sunscreens based on chromophore compounds and nanoparticles. RSC Advances, 14, 2529–2563.

113. Ramadhani, Nur Wulan, & Bintari, Sri Haryanti. (2023). Antimicrobial activity and anti-acne cream formulation of cucumber peels extract against Staphylococcus epidermidis.

114. Rizzello, L., & Pompa, P. P. (2014). Nanosilver-based antibacterial drugs and devices: Mechanisms, methodological drawbacks, and guidelines. Chemical Society Reviews, 43(5), 1501–1518.

S

115. Saeb, A. T. M., et al. (2021). FTIR analysis of green synthesized metal oxide nanoparticles: Role of plant phytochemicals as capping agents. Nanomaterials, 11(5), 1265.

116. Sahu, T., & Sahu, J. (2015). Cucumis sativus (cucumber): a review on its pharmacological activity. Journal of Applied Pharmaceutical Research, 3(1), 04-09.

117. Sankhalkar, S., & Vernekar, V. (2016). Quantitative and Qualitative analysis of Phenolic and Flavonoid content in Moringa oleifera Lam and Ocimum tenuiflorum L. Pharmacognosy research, 8(1), 16.

118. Segueni, K., et al. (2025). Evaluation of dermal wound healing potential: phytochemical characterization, anti-inflammatory, antioxidant, and antimicrobial activities of euphorbia guyoniana boiss. & reut. latex. Chem. Biodivers., Article e202402284.

119. Sharma, P., et al. (2021). Role of amino acids in wound healing and tissue regeneration. Amino Acids, 53, 1521–1538.

120. Sharma, P., et al. (2022). Green synthesis and characterization of Ag/ZnO nanocomposite using plant peel extract. Journal of Environmental Chemical Engineering, 10(3), 107456.

121. Shoukani, H. I., et al. (2024). Ciprofloxacin loaded PEG coated ZnO nanoparticles with enhanced antibacterial and wound healing effects. Scientific Reports, 14, 4689.

122. Singh, J., et al. (2018). 'Green' synthesis of metals and their oxide nanoparticles: applications for environmental remediation. Journal of Nanobiotechnology, 16, 84.

123. Sirelkhatim, Amna, et al. (2015). Review on Zinc Oxide Nanoparticles: Antibacterial Activity and Toxicity Mechanism.

124. Slinkard, K., & Singleton, V. L. (1977). Total phenol analysis: Automation and comparison with manual methods. American Journal of Enology and Viticulture, 28(1), 49-55.

125. Subramanian, S., et al. (2023). Wound healing properties of a new formulated flavonoid-rich fraction from Dodonaea viscosa Jacq. leaves extract. Frontiers in Pharmacology, 14, 1096905.

126. Swamy, K.R.M. (2023). Origin, distribution, taxonomy, botanical description, genetics, genetic diversity and breeding of cucumber (Cucumis sativus L.). International Journal of Development Research, 13(02), 61542-61559.

T & U & V

127. Tharansia Ramachandran, et al. (2024). Enhanced Wound Healing With β-Chitosan-Zinc Oxide Nanoparticles: Insights From Zebrafish Models.

128. Trinh, X.-T., et al. (2022). A comprehensive review of natural compounds for wound healing: Targeting bioactivity perspective. International Journal of Molecular Sciences, 23(17), 9573.

129. UNCTAD. (2023). Vitamin C and its antioxidant properties in biological systems.

130. Varghese, S. A., Francis, A., & Mathew, B. (2024). Metal oxide nanoparticles as anti-inflammatory agents: Mechanisms and biomedical applications. Journal of Nanobiotechnology, 22, 85.

131. Vinjamuri, S., et al. (2015). Evaluation of hemolytic activity, ATPase inhibitory activity and antitumor activity of TLC extract of lemon grass (Cymbpogon citratus). Int J Pharmacogn Phytochem Res, 7(4), 785-788.

W, X, Y, Z

132. Wali, A. F., et al. (2020). Silver nanoparticles as a potential antimicrobial agent against multidrug-resistant Pseudomonas aeruginosa. Journal of Pure and Applied Microbiology, 14(2), 1519–1525.

133. Wasef, L. G., et al. (2020). Biological activity of silver nanoparticles and their role in wound healing. Journal of Advanced Research, 21, 109–120.

134. Wei, M., et al. (2024). Role of reactive oxygen species in ultraviolet-induced photodamage of the skin. Cell Division, 19, 1.

135. Wu, G., et al. (2021). Amino acids and their roles in immune function and oxidative stress. Journal of Nutritional Biochemistry, 90, 108559.

136. Xiao, Y., et al. (2021). Zinc oxide nanoparticles for wound healing applications. International Journal of Nanomedicine, 16, 2767–2781.

137. You, C., et al. (2017). Silver nanoparticle loaded collagen/chitosan scaffolds promote wound healing via regulating fibroblast migration and macrophage activation.

138. Zeb, A. (2020). Concept, mechanism, and applications of phenolic antioxidants in foods. Food Chemistry, 312, 126–132.

139. Zhong Lu, et al. (2017). Enhanced antibacterial and wound healing activities of microporous chitosan-Ag/ZnO composite dressing. Carbohydrate Polymers, 156, 460–469.

140. Zulkefli, N., et al. (2023). Flavonoids as potential wound-healing molecules: Emphasis on pathways perspective